2017

Metatranscriptomic Analysis of Co-Occurring Phytoplankton Species in the Ross Sea Polynya

Sylvia Minjee Kim
University of Rhode Island, gtrry2500@gmail.com

METATRANSCRIPTOMIC ANALYSIS OF CO-OCCURRING PHYTOPLANKTON SPECIES IN THE ROSS SEA POLYNYA

BY

SYLVIA MINJEE KIM

A THESIS SUBMITTED IN PARTIAL FULFILLMENT OF THE REQUIREMENTS FOR THE DEGREE OF

MASTER OF SCIENCE

IN

OCEANOGRAPHY

UNIVERSITY OF RHODE ISLAND

2017

MASTER OF SCIENCE THESIS

OF

SYLVIA MINJEE KIM

APPROVED:

Major Professor Anton F. Post

Thesis Committee: Susanne Menden-Deuer

Bethany Jenkins

Nasser H. Zawia
DEAN OF THE GRADUATE SCHOOL

UNIVERSITY OF RHODE ISLAND
2017

ABSTRACT

Primary production (PP) of the Ross Sea Polynya (RSP) contributes a significant proportion of the total PP of the Southern Ocean. As a result, the photosynthetic activities of phytoplankton communities in the RSP play important roles in the overall biochemical cycling of carbon and nutrients and structuring the marine food-web. Environmental change, especially in light and iron regimes, regulates variations in PP and affects the phytoplankton community dynamics. Since individual phytoplankton species have unique nutrient requirements, the limited resources impact these algal taxa in different ways. In this study, we used metatranscriptomic analysis to examine how the algal taxa *Fragilariopsis*, *Thalassiosira*, *Pseudo-nitzschia*, *Micromonas*, and *Phaeocystis antarctica* differ in their acclimation to their shared environment during the bloom season in the RSP. During the austral spring and summer of 2013-2014, the phytoplankton communities in the RSP were iron limited across all sampling sites and exposed to high-light conditions at some sampling sites. However, the acclimation of individual algal taxa to these conditions was different. Niche partitioning between the diatom group and the haptophyte *Phaeocystis antarctica* was detected. *Phaeocystis* dominated at the greater depths (80-100m) and showed relatively low abundances at the surface (average 8.9±5.8%). *Pseudo-nitzschia* showed optimal niche adaptation among near the surface with a largest population size (average relative abundance 32.0±18.0%) and increased genetic activity. The expression of key-genes of *Pseudo-nitzschia* showed potential acclimation to limited iron and cobalamin conditions. However, the expression levels of those genes were not only controlled by the related environmental parameters, but also by a set of physical and biochemical environmental factors. Our study is limited to examining the

interaction between the phytoplankton communities and the environments. The potential effects of bacterial communities, viruses and predators should be included to further the understanding of individual algal species' niche adaptation in the future. This study demonstrates that, although some environmental factors control the overall bulk PP, those factors have variable effects on the individual algal taxon. We also show the need to consider a combination of environmental parameters to accurately predict shifts in phytoplankton community composition within the context of long-term climate change.

ACKNOWLEDGMENTS

I would like to thank my major professor Dr. Anton Post for his support and considerate guidance throughout my entire graduate student life at GSO. I also appreciate my committee members Dr. Susanne Menden-Deuer and Dr. Bethany Jenkins for their constant support and valuable input on my research. I am thankful for all team members of the Phantastic cruise in 2013-2014 with their help in providing environmental data. Special thanks go out to Dr. Tom O. Delmont for providing me with samples and offering insights in the metatranscripomic analysis. I also thank my two lab members, Rebecca Stevick and Rodrigue Spinette, for encouraging me every time with warm hearts, going through many troubleshooting exercises together, and offering from their invaluable knowledge. Finally, thank you to my family and friends in U.S. and in South Korea for being my people and sending me tremendous love.

PREFACE

This thesis was prepared using the manuscript format for submission to and according to publication guidelines of *Frontiers*.

TABLE OF CONTENTS

LIST OF TABLES

TABLE PAGE

LIST OF FIGURES

LIST OF APPENDIX FIGURES

FIGURE PAGE

Manuscript

In preparation for Submission to *Frontiers*.

Metatranscriptomic Analysis of Co-occurring Phytoplankton Species In the Ross Sea Polynya

Sylvia M. Kim

Anton F. Post*

Graduate School of Oceanography, University of Rhode Island, Narragansett, RI USA

*Corresponding author: Tel: (508) 274-5188

E-mail address: apost@fau.edu

Key Words: Ross Sea Polynya, phytoplankton community, niche adaptation, metatranscriptome

Running head: Co-occurring algal species in the Ross Sea Polynya

INTRODUCTION

As the level of CO_2 in the atmosphere has steadily increased and recently accelerated due to anthropogenic CO_2 productions (7-9 Pg C yr^{-1}), global temperatures have risen with climate change (Arrigo et al., 2008; Bazzaz, 1990; Long, 1991; Sarmiento et al., 1998; Takahashi et al., 2002). The Southern Ocean (SO, South of 50 °S) consists of only 10% of the global ocean surface, but it accounts for about 25 % of the oceanic uptake of atmospheric CO_2 (Takahashi et al., 2002, 2009). Thus, in this era, the SO has received more and more attention because of its disproportionately high and constant total primary production (~2 Pg C yr^{-1} with interannual variability of ±4%) (Arrigo et al., 2008; Le Quere et al., 2007; Moore & Abbott, 2000; Schlitzer, 2002). The SO consists of only 10% of the global ocean surface, but it accounts for about 25 % of the oceanic uptake of atmospheric CO_2 (Takahashi et al., 2002, 2009). In addition, the high biological production in the SO plays a significant role in the biochemical cycles and the biological pump process by accommodating fecal pellet formation and aggregation of particulate organic carbon (Arrigo et al., 1999; Arrigo et al., 2000; Arrigo et al., 2008; Asper & Smith, 1999; Moloney et al., 1992).

Most of the total primary production of the SO is contributed by intense phytoplankton blooms of coastal polynyas in the Antarctic during the austral spring and summer (Arrigo & van Dijken, 2003; Arrigo et al., 2015; Sullivan et al., 1993). These polynyas are recurring areas of open water surrounded by pack ice and continental shelves (Smith & Barber, 2007). After long, dark winter periods in the Antarctic, the coastal polynyas provide oases to algal communities by providing open water areas where light can penetrate and delivering nutrient supplies from sea-ice melt water as well as the upwelling of deep water masses

(Arrigo & McClain, 1994; Arrigo & van Dijken, 2003; Comiso et al., 1993). As a result, phytoplankton communities form intense blooms in these relatively fertile coastal polynyas, and their growth and biomass accumulation are much greater within polynyas than in other regions of the SO (Arrigo et al., 2000; Becquevort & Smith, 2001; Gowing et al., 2001).

Among the coastal polynyas around the Antarctic, the Ross Sea Polynya (RSP) is the largest coastal polynya (approximately 396,500 km^2) with the highest bulk primary production (~ 47.9 ± 11.6 Tg C yr^{-1}) in the SO (Arrigo & van Dijken, 2003). The RSP has significant effects on regulating regional CO_2 concentrations in the atmosphere (Arrigo et al., 2008; Le Quere et al., 2007; Sarmiento et al., 1998), controlling the local carbon cycling (Arrigo & McClain, 1994; Arrigo et al., 2000; Asper & Smith, 1999; Becquevort & Smith, 2001; DiTullio & Smith, 1995; Smith, 1995), and sustaining the local marine food-web (Giacomo R. DiTullio & Smith, 1996; Sweeney et al., 2000).

The formation and durability of the coastal polynyas are related to the combined action of latent heat, circumpolar deep water (CDW) (Fichefet & Goosse, 1999), and the strong katabatic wind (Bromwich, 1989; Bromwich & Kurtz, 1984). In the RSP specifically, the notable polynya eventually develops in December at the onset of the austral spring (Arrigo et al., 1999; Comiso et al., 1993; Smith & Gordon, 1997). The phytoplankton communities develop their blooms in early December supported by constantly improving environmental conditions (Arrigo & McClain, 1994; El-Sayed et al., 1983) and, triggered by the seeding with sea-ice algae, they follow on the heels of the ice-edge bloom (Smith & Nelson, 1986; Wilson et al., 1986). The blooms continue for several weeks to months depending on the environmental conditions and physiological properties of algal species in

the community (Arrigo et al., 1998; DiTullio et al., 2000; Smith et al., 2000). These blooms will decrease and disappear in early March when the surface water in the Ross Sea begins to refreeze.

The dynamic environmental conditions in the RSP cause spatial and temporal variations in phytoplankton growth rates and biomass in the RSP (DiTullio & Smith, 1996; Smith et al., 1996). The vertical stability of the upper water column and the extremely low concentrations of dissolved iron (DFe) of ~ 0.1 nM in the surface layer have been considered as the major factors that control the local bulk primary production in the RSP (Arrigo et al., 2015; Bertrand et al., 2011; Gerringa et al., 2015; Martin et al., 1990; Sedwick et al., 2000; Sverdrup, 1947; Zhu Z et al., 2016). In addition, grazing by zooplankton (Deibel & Daly, 2007; Lancelot et al., 1993), seeding by the sea ice algae (Asper & Smith, 1999; Smith & Nelson, 1985; Smith & Nelson, 1986), and the light limitation due to sea ice cover or continental shelf shading (Arrigo et al., 2000; Perovich, 1990; Smith & Gordon, 1997) may also control the biological productivity of phytoplankton communities in the RSP.

Spatial and temporal variations in the composition of phytoplankton communities in the RSP have been reported. These communities are typically dominated by the haptophyte *Phaeocystis antarctica* during the spring and early summer when the mixed layer in deep, and several diatom species (*Pseudo-nitzschia*, *Fragilariopsis*, *Thalassiosira*, *Chaetoceros*) become more abundant in late summer and coincide with a shallower mixed layer depth (Delmont et al., (*in prep*); Smith et al., 2000; Tremblay & Smith., 2007). Some studies have presented that iron and light availability (Bertrand et al., 2011; Delmont et al., (*in prep*); Sedwick et al., 2000; Sverdrup, 1947), water stratification (Rozema et al., 2016) and temperature (Zhu Z et al., 2016) might be the major factors that control the

relative abundance of individual algal species in the RSP during the bloom periods. However, few studies conducted in the RSP investigate how several different species can co-occur in the same limited environmental conditions. Analysis of ecological and physiological status of individual algal species would further our understanding about algal species' relative contributions to bulk primary production in the RSP, in terms of co-existence and characterization of their niches. It is also important for better predictions of changes in the phytoplankton community structure in response to long-term environmental change.

The main objectives of this research were 1) to examine how individual algal taxon (*Fragilariopsis*, *Thalassiosira*, *Pseudo-nitzschia*, *Phaeocystis*, and the prasinophyte *Micromonas*) respond to their ambient environmental conditions and 2) to estimate the ecological properties of each algal taxon in the phytoplankton community in the RSP. We employed a total of six metatranscriptomes collected from six different stations in the RSP during the project: Phaeocystis antarctica adaptive responses in the Antarctic ecosystem (Phantasic) onboard the R/V Nathaniel B. Palmer during the austral spring and summer 2013-2014. Using metatranscriptomic analyses, we report the effects of common environmental conditions (e.g. physical parameters: temperature, salinity and light intensity) and biochemical factors (dissolved inorganic macronutrients and dissolved iron) on the genetic responses and potential metabolic acclimations of co-occurring individual algal taxon.

MATERIALS AND METHODS

Sampling

Cruise NBP13-10 of the R/V Nathaniel B. Palmer explored the Ross Sea Polynya (RSP) during the first research cruise of the Phantastic project in the

austral spring and summer period, from December 2013 to January 2014. Here, we report on geochemical, biological and transcriptome data for surface layer (10 m depth) samples from 6 stations (1, 2, 3, 4, 5, and 6). These samples were taken between December 24, 2013 and January 4, 2014 within the RSP (Fig. 1). Samplings at station 1 and 2 were conducted at approximately 9:00 GMT and 1:00 GMT respectively. Samplings at the remainder of the stations were performed around 18:45 GMT.

Hydrographic profiles (temperature, salinity and light irradiance) and water samples for phytoplankton pigment analysis via high performance liquid chromatography (HPLC) and plankton community composition analysis via FlowCAM were obtained from each station by a conventional shipboard conductivity-temperature-depth (CTD) sensor and 12 x 10L Niskin bottle rosette sampler. Water samples for metatranscriptomic analysis, dissolved iron (DFe) and major nutrient analyses (NO_2/NO_3, and PO_4) were also collected from each station using modified 12 L GO-FLO (Oceanics) samplers offered by the Royal NIOZ (The Netherlands) which were attached to a Trace Metal Clean (TMC) frame provided by the United States Antarctic Program.

Metatranscriptomic analyses

Water samples (4.0 – 8.0 L depending on the biomass) for metatranscriptomic analysis were rapidly filtered onto 0.2 μm filters using a vacuum pump, and the total filtration process took 30 minutes or less for each sample. The six filters were flash frozen in liquid nitrogen and stored at -80 ˚C prior to RNA extraction.

RNA extraction, library preparation, and sequencing

Total RNA was extracted from each filter (total 6) using a modified RNAprotect-Bacteria-Reagent-Handbook protocol 5 and 7 using the RNeasy Mini kit (Qiagen). The volumes of i) the acid-washed glass beads (0.1 mm), ii) TE buffer solution, and iii) RLT buffer solution were increased to optimize the yield of total RNA on the cell lysis step; to 30 mg for the acid-washed glass beads (0.1mm), to 300ul for TE buffer solution, and to 1050 µl for RLT buffer solution. Extracted RNA was qualified and quantified spectrophotometrically with a Nanodrop (Thermo Fisher) instrument; the acceptable purity ratio was defined as A260/A280 ratio of 2.0-2.3 and A260/A230 ratio of 1.8-2.2 (Desjardins & Conklin, 2010). Polyadenylated messenger RNA (mRNA) from the extracted total RNA was enriched using the MagJET mRNA Enrichment Kit (Thermo Scientific) following the manufacturer's standard protocol and mRNA was quantified using a Qubit® fluorometer. RNA-Seq libraries were prepared using the ScriptSeq v2 RNA-Seq Library Preparation Kit (Epicentre); cDNA was synthesized according to the manufacturer's official protocol, barcodes and Illumina adaptors were added to the synthesized cDNA fragment ends, and the cDNA fragments were amplified over a total 18 polymerase chain reaction (PCR) cycles. The six prepared RNA-Seq libraries were qualified and quantified on HS DNA chips using the Agilent Bioanalyzer 2100. The RNA-Seq libraries then were sized-selected using a Pippin Prep™ electrophoresis platform and quantified by qPCR before sequencing. The size-selected RNA-Seq libraries (average insert size: 225-287 bp) were subjected to paired-end sequencing on the NextSeq Illumina platform with a Mid-Throughput Kit in the Keck sequencing facility at the Marine Biological

Laboratory, Woods Hole, MA. Barcoding (from RNA-Seq library prep stage, Epicentre) was used to identify the different samples during post-run analyses.

RNA-Seq data analysis

Based on the Phred quality scores generated during the sequencing run, the raw reads were trimmed for the quality by Trimmomatic 0.36 (Bolger et al., 2014) in the paired end mode with parameters AVGQUAL 30 and CROP 134. Reference-based assembly was performed using Bowtie2 (Langmead & Salzberg, 2012); quality filtered reads of each metatranscriptome were mapped against the *Fragillariopsis*, *Pseudo-nitzschia*, *Thalassiosira*, *Micromonas* whole genomes and *Phaeocystis* transcriptome as the reference genomes. *Fragillariopsis cylindrus* CCMP1102 (Mock et al., 2017), *Thalassiosira oceanica* (Lommer et al., 2012), and *Micromonas* sp. ASP10-01a (BioProject: PRJNA276743) whole genomes were obtained from NCBI genome database, and *Pseudo-nitzschia antarctica* genome, and *P. antarctica* strain CCMP 1374 (Delmont et al., under submission) transcriptome were provided from previous studies in our group. TPM (transcripts per million) were calculated with the counts of mapped reads to normalize the overall alignments for different genome lengths and the library sizes.

$$\frac{The\ count\ of\ mapped\ reads\ from\ a\ metatranscriptome}{The\ length\ of\ the\ reference\ genome\ (Kb)} = x$$

$$x/\sum x\ (total\ six\ metatranscriptomes)\ (Mb) = TPM\ (Transcripts\ per\ million)$$

The visualization of distributions of reads on the reference genomes was performed with Anvi'o (Eren et al., 2015). ORFs of each reference genomes were predicted with prodigal (Hyatt et al., 2010) and predicted ORFs were transformed

to protein sequences and they were functionally annotated using COGs database (Tatusov et al., 2000) with Blastp e-value threshold 1e-5. The coverage of predicted genes in each reference genome were calculated by

$$\frac{\sum coverage\ of\ each\ bp\ in\ gene}{gene\ length}$$

Filtration excluded the lowly expressed (low-coverage) genes with 'cpm' function (cpm < 0.5) in edgeR (Robinson et al., 2010), and also the genes for which had mapped reads from less than 3 samples were excluded. The filtered data were normalized and tested for the differentially expressed genes using the "R" with edgeR package (Robinson et al., 2010) and limma package (Ritchie et al., 2015). 'calcNormFactors' function for TMM normalization (Robinson & Oshlack, 2010) in edgeR was used to calculate the normalization factors relying on the library sizes and the composition bias; TMM normalization method reduces impacts of changes in species abundances on estimating gene expression by assumption that expression of a large proportion of genes in a certain organism un-change regardless the changes in environmental conditions. The calculated normalization factors were used during testing the differentially expressed genes through 'voom' function in limma (Law et al., 2014). 'Voom' function first adjusted the bias between the samples using the calculated normalization factors. This function also estimated the mean-variance relationship of the log-counts and calculated a precision weight for each sample. Processed data then was entered to the empirical Bayes analysis pipeline stored in limma package (Law et al., 2014; Phipson et al., 2016) to analyze the differential gene expression. Multidimensional plot (MDS)

for investigating the differences in global gene expression patterns between the samples was produced with limma package on "R". The 100 most variable genes were also predicted. Based on the published papers, the genes that are related to the iron and light variations were extracted from the functional profiles of each reference genome mapping (key-genes). We used STAMP (Parks et al., 2014) software to show the differential expression levels of selected-genes (key-genes) across the samples for each reference species with heat maps and to estimate the correlation between the key-genes expression levels and the environmental parameters.

Phytoplankton pigment analysis via HPLC

Pigment HPLC analysis was performed by Kate Lowry and Kate Lewis at Stanford Woods Institute. The water samples for the HPLC analyses were filtered through Whatman glass-fiber filter (GF/F) with a nominal pore size of 0.7 μm (< 150 mm Hg). The pigment samples were immediately frozen in liquid nitrogen after filtration and stored at -80 ˚C until HPLC analysis. Phytoplankton pigments were extracted in 90 % acetone, and they filtered through 0.45 μm HPLC syringe cartridge into a 2 mL amber crimp-top vial. The filtered samples were injected into the HPLC system and the pigments were identified based on comparisons of their in-line diode array detector absorbance spectra. Standards were either purchased or fraction collected from algal monocultures. Calculating taxonomic composition of phytoplankton community from the HPLC data were performed with Chemtax version 1.95 (Wright, 2008).

Phytoplankton species characterization by FlowCAM

The FlowCAM was used to estimate the community composition at daily station (onboard) by Hannah Joy-Warren (Stanford University). Two

magnifications (40x and 100x) were used for imaging the samples. Samples imaged with the 4x objective lens were run using a 300 μm flow cell, and samples imaged with the 10x objective were run on a 200 μm flow cell. The FlowCAM data provided an estimated relative abundance (%) of Green algae, Cryptophytes, Diatom species, Haptophytes, and Dinoflagellate.

Dissolved Iron (DFe) and major nutrient measurements

Dissolved Iron (DFe) and major nutrient data were provided by Dr. Loes J. A. Gerringa, Patrick Laan and Dr. Hein J.W. De Baar from Netherlands Institute for Sea Research (NIOZ), following the protocols published in Gerringa et al. 2015. Sample handling and filtrations were done inside the trace metal van under clean conditions with Sartorius® 0.2 μm for DFe and Satrobran 300 μm for major nutrients, respectively. DFe concentrations were measured directly on board following an automated Flow Injection Analysis method (Klunder et al., 2011). Samples were analyzed in triplicate and standard deviations were on average 2.8%. Blanks were determined daily by loading a low iron seawater sample for 0, 5, 10 seconds. The blank values ranged from not detectable up to 14 pM. The average limit of detection, 16 pM was defined as 3 times the standard deviation of the mean blank and measured daily. Filtered and acidified (Seastar© baseline hydrochloric acid; pH 1.7) seawater was concentrated on a column containing aminodiacetid acid (IDA) which binds only transition metals and not the interfering salts. The column was rinsed with ultra-pure water, and eluted with diluted acid. After mixing with luminol, peroxide and ammonium, the oxidation of luminol with peroxide was catalyzed by iron and a blue light is produced and detected with a photon counter. The concentration of iron was calculated using a standard

calibration line, where a known amount of iron was added to low iron containing seawater. Using this calibration line a number of counts per nM DFe is obtained.

Satellite remote sensing

Satellite remote sensing data was provided as a compressed kml format (kmz) via email during the cruise by an automated system at Stanford University under the supervision of Dr. Gert van Dijken.

The MODIS/Aqua ocean color satellite scenes were downloaded every 3 hours from NASA ftp-servers through two near real-time subscriptions using the NASA Ocean Biology Processing Group's data subscription service. The chlorophyll products were extracted from the downloaded files and mapped to a common projection. In addition, ice concentration data was downloaded from the National Snow & Ice Data Center (NSIDC) and re-projected in the same way.

RESULTS

General Environmental Conditions at each Sampling Site

The surface area of the Ross Sea Polynya (RSP) increases in size throughout the austral spring-summer sampling period (Fig. 2). The rise in sea surface temperature (from -1.08 ˚C to 0.67 ˚C) during the sampling period is indicative of the solar warming of surface waters, resulting in melting of the surrounding sea ice and expansion of the RSP. Temperatures lower than 0 ˚C were measured at the earlier sampling stations (1, 2, 3) within the Central RSP transect, and temperatures above 0 ˚C were detected at the later sampling stations (4, 5, 6) along the Western RSP transect (Fig. 1; Table 1).

A phytoplankton spring bloom was detected in the RSP throughout the sampling period, indicated by relatively high phytoplankton biomass and chlorophyll *a* (chl *a*) concentrations of >5 µg L^{-1} (data not shown). High chl-*a* concentrations were observed along the Ross Ice Shelf and decreased with increasing distance from the shelf (Fig. 2). Based on corresponding data from FlowCAM, HPLC pigment, and 18S diatom community analyses (Filliger, unpublished), the phytoplankton communities at the surface (10 m) were dominated by several diatom species, particularly *Pseudo-nitzschia* (Fig. 4b, 4c and Fig. 5b). The haptophyte *Phaeocystis antarctica*, commonly found in the RSP, showed relatively low abundance within the phytoplankton communities at the surface, but their abundance increased at greater depths at all sampling sites (Fig. 4b, 4c and Appendix 2). The highest chl-*a* concentration (6.51 ± 0.06 µg L^{-1}) and fluorescence measurements (16.75 AU) were observed at station 4 where the highest relative abundance of *Pseudo-nitzschia* was detected (Table 1; Fig. 5b).

Higher chl-*a* concentrations and fluorescence measurements corresponded with lower Photosynthetically Active Radiation (PAR) (Table 1; Fig. 3).

The concentrations of nitrite/nitrate and phosphate were similar across the sampling sties, with average concentrations of 20.0 ± 0.75 µM and 1.39 ± 0.19 µM, respectively (Table 1). Based on the Redfield ratio (N/P~16) (Redfield, 1958), only station 4 showed potentially P-limited environmental conditions, whereas the remainder of the stations had ratios indicative of N-limited conditions (Table 1).

In general, the concentration of dissolved iron (DFe) was extremely low at the surface throughout the RSP during the cruise (<0.10 nM) (Gerringa et al., 2015). The average DFe concentration at sampling sites 1, 2, 4, 5, and 6 was 0.05 ± 0.01 nM. The DFe concentration at station 3 was much higher than the others, with a concentration of 0.2 ± 0.003 nM (Table 1). Gerringa et al. (2015) interpreted the higher DFe concentration at station 3 as an indication of iron input at the surface originating from dust deposition or melting sea ice. These processes were also suggested as the explanation of lower salinity at station 3 (Table 1).

Evaluation of Metatranscriptomic Libraries

To examine the genetic response of individual algal species (*Fragilariopsis*, *Thalassiosira*, *Pseudo-nitzschia*, *Macromonas*, and *Phaeocystis*) to their shared environmental conditions in the RSP, we sequenced metatranscriptomes for each sampling site. The total yield of extracted RNA from each sample varied from 128.5 to 745.9 ng μL^{-1}. From this extracted total RNA, messenger RNA (mRNA) was enriched for each sample, yielding 0.066 ± 0.014 ng μL^{-1} to 1.621 ± 0.026 ng μL^{-1} (Table 2). The percentage of mRNA among the total RNA was less than 0.1% in samples 1 and 2, and more than 0.1% in the remainder of the samples (Table 2). The number of quality controlled reads varied from 326,364 to 31,307,197 and had

an average GC content of 48%; the metatranscriptomic libraries for stations 1 and 2 have 326,364 reads and 427,800 reads respectively, while metatranscriptomes for the other stations yielded more than 23,000,000 reads (Table 4).

Selection of the Reference Genomes

In order to select genomes for reference-based mapping, we compared several phytoplankton genomes and transcriptomes from a variety of original sampling locations and culture conditions to the overall alignments with our transcriptomes. The candidate algal taxa for reference genome selection were determined from inspection of phytoplankton communities in the RSP during our cruise period by FlowCAM, HPLC pigment, and 18S diatom community analyses (Filliger, unpublished) (Fig. 4b, 4c and Fig. 5b) and from publications on phytoplankton communities in the RSP during the bloom period (Delmont et al., (*in prep*); Smith et al., 2000; Tremblay & Smith., 2007). As a result, we included *Fragilariopsis* sp., *Thalassiosira* sp., *Pseudo-nitzschia* sp., *Micromonas* sp. and *Phaeocystis antarctica* reference genomes and transcriptomes for downstream metatranscriptome analysis (Table 3).

All reference genomes and transcriptomes of *Fragilariopsis* sp. were from samples collected in the Southern Ocean (*Fragilariopsis-kerguelensis*-L2_C3 (MMETSP; (Keeling et al., 2014)), *Fragilariopsis-kerguelensis*-L26_C5 (MMETSP), *Fragilariopsis cylindrus* CCMP1102 (NCBI; (Mock et al., 2017)). The overall alignments from our metatranscriptomes between the three different genomes and transcriptomes of *Fragilariopsis* sp. were similar across the samples (Table 4). Overall alignments to three different *Thalassiosira* sp. genomes and transcriptome were also similar across the samples, although the culture conditions of these reference *Thalassiosira* sp. were different. *Thalassiosira-antarctica-*

CCMP982 (MMETSP) and *Thalassiosira oceanica* (NCBI, (Lommer et al., 2012)) were cultured under iron-limited conditions, whereas *Thalassiosira pseudonana* CCMP1335 (NCBI, (Armbrust, 2004)), known as a coastal species, was originally isolated from Moriches Bay and continuously grew in culture before DNA extraction.

The overall alignments of the metatranscriptome reads with *Pseudo-nitzschia* sp. and *Micromonas* sp. were different for the different reference genomes and transcriptomes available for these genera. Across all samples, an average of 50.0 ± 16.3% and 11.4 ± 5.9% of the reads aligned to *Pseudo-nitzschia antarctica* and *Pseudo-nitzschia australis*, respectively. The *Pseudo-nitzschia antarctica* genome was reconstructed from samples obtained in the RSP whereas the *Pseudo-nitzschia-australis*-10249_10_AB transcriptome (MMETSP) was reconstructed from samples obtained in Monterey Bay, CA. In the case of *Micromonas* sp., the transcriptomes (*Micromonas*-sp-CCMP2099, sp-NEPCC29, sp-RCC472 (MMETSP)), which were not from the Antarctic, yielded a higher degree of alignment than the genome from the Amundsen Sea Polynya (ASP), Antarctica (*Micromonas* sp. ASP10-01a). For *Phaeocystis antarctica* (*P. antarctica*), only one source was available from the previous study in our group (Delmont et al., (*in prep*)).

Based on the original locations and cultured environmental conditions of these references, we selected *Fragilariopsis cylindrus* CCMP1102 (*F. cylindrus*), *Thalassiosira oceanica* (*T. oceanica*), *Pseudo-nitzschia antarctica* (*P. nitzschia antarctica*), *Micromonas* sp. ASP10-01a (*Micromonas*), *Phaeocystis antarctica* (*P. antarctica*) as reference genomes and transcriptomes in this study.

Reference Genome Mapping

Of the total reads, 26.7 % (sample 1), 47.0 % (sample 2), 41.5 % (sample 3), 45.5 % (sample 4), 17.1 % (sample 5), and 22.7 % (sample 6) did not map to any of the reference genomes/transcriptomes (Table 5). *P. nitzschia antarctica* displayed the highest alignment percentage with the reference genomes across all metatranscriptome libraries. From the individual libraries, 35.8 % (sample 1), 34.4 % (sample 2), 46.8 % (sample 3), 43.0 % (sample 4), 73.7 % (sample 5), and 66.2 % (sample 6) of the reads aligned to the *P. nitzschia antarctica* genome (Table 5). The relatively high alignment of reads to the *P. nitzschia antarctica* genome is in agreement with the algal community metatranscriptomic analysis of the on-deck incubation experiments completed during the same cruise (Delmont et al., (*in prep*)). Overall alignment percentages to the two other selected diatom genomes varied from 1.6% to 19.6% of the total reads from individual libraries. Less than or equal to 0.4 % of reads from individual libraries mapped to *P. antarctica* and *Micromonas* (Table 5).

The Correlation between Read Alignments and Relative Abundances

We normalized the overall alignments to each reference genome to 100% across individual libraries (not including un-mapped reads) by calculating Transcripts Per Kilobase Million (TPM). Calculated TPM were used to examine if, in each sample, the percentage of overall alignment of assembled transcripts to an algal reference genome correlated with the relative abundance of that same taxon in the phytoplankton community. Higher TPM values of diatom species corresponded with the diatom-dominated phytoplankton communities in the same RSP samples during austral spring and summer in 2013-2014 as determined by FlowCAM and HPLC pigment analyses (Fig. 4b and 4c). However, there was no

clear agreement between the read alignments (TPM) to each diatom species shown here and the relative abundance of individual diatom species determined by 18S diatom community data (Filliger, unpublished) (Fig. 5). The relative TPM values to each diatom species changed regardless of the changes in their relative abundances within the diatom community. The TPM value of *P. nitzschia antarctica* increased whereas the TPM value of *F. cylindrus* and *T. oceanica* decreased over the sampling period (Fig. 5a). The changes in the relative abundances of haptophytes and chlorophytes in the phytoplankton communities across the samples were also not correlated with TPM values of *P. antarctica* and *Micromonas* (Fig. 4).

Global Gene Expression Patterns

Reads that mapped to *P. nitzschia antarctica* and *F. cylindrus* were evenly distributed over their reference genomes whereas reads mapping to other species were concentrated on partial areas of the whole genome (Fig. 6). Since the number of mapped reads affiliated with each species were not evenly distributed between the samples (Fig. 6, box plots), we converted the coverage values of predicted genes of each reference genome to cpm (counts-per-milion), which normalized the different sequencing depths, to compare the differences between the samples. The differences in global gene expression patterns of each algal species across the sampling sites were examined with multidimensional scaling (MDS) plots; each sample site has different environmental and geographical conditions (Table 1; Fig. 1 and Fig. 2). Since stations 1 and 2 have lower quantity and quality metatranscriptome reads, which might cause a significant bias in the MDS plots (e.g. Appendix 1), we used only the metatranscriptomes of stations 3, 4, 5 and 6 for further analyses (Fig. 7). The overall gene expression patterns of *P. nitzschia*

antarctica and *P. antarctica* were relatively similar at stations 5 and 6 and different at stations 3 and 4 (Fig. 7a and 7c). On the other hand, the global gene expression patterns of *T. oceanica* and *Micromonas* were similar for stations 3 and 4 (Fig. 7d and 7e). *F. cylindrus* showed different gene expression patterns across all samples (Fig. 7b).

Expression Patterns of Key Genes

Since the environmental conditions across the sampling sites were not significantly different, we expected that there would be no remarkable shifts in gene expression. Transcripts for the 100 most variable predicted genes from all reference species were examined to determine if these genes were closely linked to environmental factors. These genes did not change expression levels according to the environmental conditions or they were unannotated. This implies that the environmental conditions between the sampling sites were too similar to elicit a significant difference in transcript abundance of the genes related to the environmental parameters. In a next step, we examined how the phytoplankton communities responded to their environmental conditions, particularly to iron and light regimes and cobalamin availability between the samples. Based on the literature, we determined a set of key-genes that are differentially expressed under varying iron and light conditions and concentrations of cobalamin in these phytoplankton taxa (Fig. 8). Transcript abundances for the chlorophyte *Micromonas* were too low to determine difference in expression levels of these key genes. The overall coverage of key-genes before the normalization was highest for *P. nitzschia antarctica* (Fig. 8).

To determine the differential expression patterns of key-genes between samples, we applied TMM normalization (Robinson & Oshlack, 2010) and limma

empirical Bayes analysis pipeline (Law et al., 2014). The key-gene expression patterns were not significantly different across the sampling sties, but they were different for the individual species (Fig. 9). Overall, key-gene expression patterns of *T. oceanica* and *P. antarctica* were similar. The few key-genes that were differentially expressed were related to vitamin B_{12} (cobalamin) biosynthesis and to iron stress response (Flavodoxin) in the functional profiles of *T. oceanica* and *P. antarctica*. Overall cobalamin biosynthesis genes showed a low transcript abundance, but the Flavodoxin transcript abundances was distinctly higher for stations 5 and 6 (Fig. 8), suggesting that iron limiting conditions may have prevailed for these taxa at the two locations. Transcript abundances for *F. cylindrus* and *P. nitzschia antarctica* indicated a greater number of differentially expressed key-genes than was found in *T. oceanica* and *P. antarctica*, but expression levels for each gene were distinctly different for these two species (Fig. 8 and Fig. 9). Genes involved in low light acclimation (Plastocyanin, Photosystem II stabilization factor) were most prominently expressed in *F. cylindrus*, whereas transcript abundances for iron stress related genes (Flavodoxin, Ferredoxin, Rieske protein etc.) were much higher in *P.nitzschia antarctica*.

Flavodoxin was highly expressed in all species except *Micromonas*. Plastocyanin was expressed only in the pennate diatoms *T. oceanica* and *F. cylindrus*. Gene expression for multicopper oxidase, a predicted ferric reductase, a putative heme iron utilization, and a heat shock protein was specific to *P. nitzschia antarctica* (Fig. 9). Genes for cobalamin biosynthesis protein were highly expressed in all species except *Micromonas*. The methionine synthase I (cobalamin-dependent) gene was shown in the functional profiles of *P. antarctica*,

F. cylindrus, and *P. nitzschia antarctica*, and transcripts for methionine synthase II (cobalamin-independent) were detected only in *F. cylindrus* (Fig. 9).

Since the RSP metatranscriptomes were highly dominated by transcripts of *P. nitzschia antarctica* (~50% of total reads) (Fig. 4a and Fig. 6c), we further analyzed the key-genes expression levels of *P. nitzschia antarctica* between the sampling sites. Figure 10 shows the same heat map as Fig. 9 (*P. nitzschia antarctica*) in descending order of mean gene expression levels in a log2 scale across the samples. We determined that the key-genes expression patterns were more similar between stations 5 and 6 (Fig. 10), a pattern that was also observed for the global gene expression patterns of *P. nitzschia antarctica* (Fig. 7c). Altogether, genes that encode components of the photosynthetic apparatus and that are involved in light acclimation responses were amongst the most highly expressed genes, whereas genes implicated in Fe-dependent redox processes were much less expressed (Fig. 10). These findings suggest that *Pseudo-nitzschia* was acclimated to low light rather than to nutrient (specifically iron) limitation.

We further compared transcript abundances of the key-genes for their correlation with environmental parameters, leading to sometimes surprising observations. The genes of deoxyribodipyrimidine photolyase, ferredoxin-NADP reductase, and NADPH-dependent glutamate synthase beta chain correlated with variations in temperature and salinity, whereas the Mg-chelatase subunit ChlD gene had an inverse correlation with these variables (Table 6). Transcript abundances for the genes encoding 6-phosphofructokinase, cobalamin biosynthesis protein CobN, and Mg-chelatase were positively correlated with DFe concentrations, but where inversely correlated with chl-*a* concentrations and with the relative abundance of *Pseudo-nitzschia* in phytoplankton communities (Table

6). The genes related to carbon fixation (Fructose-bisphosphate aldolase class 1 and Photosystem II stability/assembly factor) were inversely correlated with light intensity (Table 6).

DISCUSSION

The "paradox of the plankton" postulate (Hutchison, 1961) states that many phytoplankton species coexist since they compete for the same resources in constantly changing environments. However, the phytoplankton community is sometimes dominated by one taxon, which usually happens during the summer blooms when the water layers are stratified and the environmental conditions do not change as quickly as in other seasons. In the case of the phytoplankton communities in the RSP, they only flourish throughout the austral spring and summer when dissolved iron is supplied by dust deposition and sea ice melting, and light reaches below the surface. Several algal taxa that often co-occur (Arrigo et al., 1999; DiTullio & Smith, 1996; Smith et al., 2000), participated in the intense RSP phytoplankton bloom studied in this thesis. The seasonal variations in iron, light and water stratification have been considered as major limited resources controlling the bulk primary production (Bertrand et al., 2011; Delmont et al., (*in prep*); Sedwick et al., 2000). Closer to the peak of the summer season, the environmental conditions of the RSP became more uniform; water masses were more stratified because of ice melt water (less salty) and increasing sea surface temperature due to stronger solar radiation; the dissolved iron were limited throughout the RSP (Boyd, 2002; Smith et al., 2014). As a result, reduced variations in environmental factors near the surface would causes increased competition between the phytoplankton species for limited resources. However,

how those limited environmental resources interact with the physiological and ecological properties of individual algal species in the phytoplankton community is less well understood. Additionally, different algal taxa have different C:N:P ratio as well as different iron requirements, resulting in differences in how these taxa responds to environmental stressors (Alexander et al., 2015) and affecting the contribution that each species makes to primary production (Arrigo et al., 1999; Arrigo et al., 2000; Smith & Asper, 2001). These responses are mediated via the expression of genes that drive acclimation to changing nutrient and light regimes. Thus, environmental conditions likely control the relative abundance of individual algal species and their contribution to primary productivity by adjusting their growth requirements via the expression of stress response genes (Arrigo et al., 1999; Delmont et al., (*in prep*).; Tagliabue & Arrigo, 2005).

During the blooms in the RSP, the phytoplankton community often consists of several diatom species and the haptophyte *Phaeocystis antarctica* (Delmont et al., (*in prep*); Sweeney et al., 2000). *P. antarctica* is the first species to form a bloom in spring followed by an extensive diatom blooms in summer (Smith et al., 2000; Tremblay & Smith., 2007). Based on culture studies, *P. antarctica* grows better under low iron and low irradiance conditions than diatom species, and after iron input or light level change, the growth rate of *P. antarctica* change more significantly than diatom species (Coale et al., 2003; Sedwick et al., 2000). *P. antarctica* also showed higher efficiency in converting carbon dioxide to organic carbon via photosynthesis (Arrigo et al., 2000; Sweeney et al., 2000; Tagliabue & Arrigo, 2005). These studies suggested a potential role for iron and light regimes in regulating the relative abundances of individual algal taxon within the phytoplankton community. However, in the ocean, there are more environmental

variables than just iron and light and they often have opposite gradients. The responses of individual algal species to their ambient environmental conditions would not necessarily be the same as found in culture experiments. Thus, knowledge on how environmental gradients in the ocean are reflected in the ecology of phytoplankton communities can also predict future shifts in the phytoplankton community composition in response to climate change. Metatranscriptomic analyses allow the study of how individual algal species within a phytoplankton community perceive their shared environment and acclimate to optimize their performance. Here we investigated the potential niche adaptation of individual algal taxon in the RSP by employing metatranscriptomic analyses and correlating these with environmental and biological data.

Iron-limited conditions were identified across all sampling stations during the austral spring and summer in 2013-2014. The phytoplankton communities at stations 3 and 6 were also acclimated to high-light conditions. We found that chl-*a* concentrations and chlorophyll fluorescence were inversely correlated with Photosynthetically Active Radiation (PAR) (Fig. 3). Chl-*a* concentrations and fluorescence are often used indicators of photosynthetic biomass (Cullen, 1982; Falkowski & Kiefer, 1985; Steele, 1962). Therefore, lower chl-*a* concentrations and fluorescence values at higher Photosynthetically Active Radiation (PAR) would indicate that some populations in the phytoplankton communities at the surface had acclimated by reducing their pigment content to avoid photoinhibition (van Hilst & Smith, 2002). This was also in agreement with the analysis of the maximum efficiency of the photosystem II (PSII) (Fv/Fm) by a PAM fluorometer of the on-deck incubation experiments performed during the same cruise (Alderkamp et al, (*in prep*)). The changes in expression levels of gene encoding

photosystem II stability/assembly factor depending on the Photosynthetically Active Radiation (PAR) (Table. 5) also supported the potential effect of photoinhibition on the phytoplankton communities. Also, abundant transcripts of the flavodoxin genes, usually expressed under iron-limited condition as this molecule replaces ferredoxin in the photosynthetic process (McKay et al., 1997; McKay et al., 1999; Morrissey & Bowler, 2012; Palenik, 2015), were detected in all species, except *Micomonas*. This could indicate that phytoplankton communities were responding to iron-deficient condition.

Looking into further detail, even though phytoplankton communities thrived under the same environmental conditions at each station, individual algal taxa had different relative abundances and exhibited different acclimation characteristics to the shared environment. During the austral spring and summer 2013-2014 sampling period in, the phytoplankton communities at the surface in the RSP were highly dominated by pennate diatom taxa, especially *Pseudo-nitzschia* sp. The haptophyte *P. antarctica*, the species that usually dominates in the RSP during the bloom season (Delmont et al., (*in prep*); Smith et al., 2000; Tremblay & Smith., 2007), had relatively low abundances near the surface. However, vertical profiles of FlowCAM data identified that the relative abundance of *P. antarctica* increased with increasing water depth and relative abundances of diatom groups decreased (Appendix 2). The distributions of diatom species and *P. antarctica* in the water column may reflect on the hydrographic conditions during this season. This is because phytoplankton communities in shallow mixed layers or more stable water are often dominated by diatoms whereas deeper mixed layer or relatively unstable water columns are often dominated by *P. antarctica* in the RSP (Arrigo et al., 1998; Goffart et al., 2000; Smith & Asper, 2001). An alternative interpretation

could be that bacterial community composition changed with depth. Many algal taxa are auxotrophic for cobalamin (vitamin B12 dependent) and often this compound is provided by bacteria (Bertrand et al., 2015; Delmont et al., 2014; Shields & Smith, 2008). The fact that cobalamin biosynthesis genes were abundantly transcribed for the taxa that mapped to reference genomes, is an indication that cobalamin was a limiting factor for the phytoplankton community at large.

Different relative abundance of each algal species in the phytoplankton communities at each station correlated with the variations in their responses to environmental stressors as indicated by their genetic acclimation. First of all, the metatranscriptomes of the phytoplankton communities in the RSP contained an abundance of diatom transcripts that mapped to different diatom reference genomes. This finding is consistent with data obtained from FlowCAM and HPLC pigment analyses (Fig. 4). However, upon further inspection, the proportion of the reads affiliated with the three different diatom species in our metatranscriptomes did not match their relative abundance in the phytoplankton community as determined with 18S sequencing of diatom communities at the same sites (Filliger, unpublished) (Fig. 5). There are a few reasons why 18S sequence data do not match read abundances in metatranscriptomes. Firstly, the difference in the water samples for the metatranscriptomic analysis and the 18S sequencing analysis could cause this mismatch, since their samples were not collected from the same rosette samplers. Another reason is that different taxa may have different 18S gene copies per cell thereby skewing the contribution each taxon makes to the community and its metatranscriptome. Also, transcript abundance may change with the growth phase of the taxon; typically fast growing populations have higher transcriptional

activity then do populations that enter stationary phase. The mismatch may further be due to the differences and inconsistencies between the genetic make-up of the taxa in each sample and their matching genomes in the reference database used for each analysis.

We used MDS plots of each algal species across the sampling sites to examine whether environmental conditions at each of the sampling sites affected the global gene expression patterns of individual species. *Micromonas* and *T. oceanica* showed similar global gene expression patterns at sampling stations 3 and 4, while *P. antarctica* and *P. nitzschia antarctica* presented similar global gene expression patterns at sampling stations 5 and 6 (Fig. 7). However, these changes in the global gene expression patterns between the sampling sites were not driven by differential expression of the genes that are involved in acclimation responses. None of the transcripts of 100 most variable predicted genes for each algal taxon were linked to known environmental stress responses. However, we cannot exclude that these may be as yet unannotated genes as the limited databases of eukaryotic algae still leave us with significant knowledge gaps. Based on the available results, we concluded that the variations in the environmental factors between the sampling sites were not sufficiently distinct that they would cause remarkable changes in global gene expression patterns. Rather, the differences and similarities shown in the global gene expression patterns reflected response to minor changes over a set of environmental conditions, not a clear cut response to a specific environmental factor.

To examine how individual algal species responded to their shared environment, we extracted the key-genes associated with major limited environmental factors, such as light and iron regimes that control primary

production in the RSP (Sedwick et al., 2000). As expected, since there were no significant changes in the environmental conditions between the sampling sites, no notable shifts in the overall key-genes expression patterns of each species were detected (Fig. 9). Instead, the expression patterns for these key-genes were characteristic for the individual species. Flavodoxin, one of the key-genes expressed under the iron-deficient condition as a replacement for ferredoxin under iron limiting conditions (McKay et al., 1997; Palenik, 2015), was commonly expressed in the functional profiles of all species, except *Micromonas*. As we mentioned above, this indicates, with the once exception, all species had been exposed to iron-limitation and their acclimation response is shown from high transcript abundance of the flavodoxin gene. The differences in transcript abundance between flavodoxin and ferredoxin genes were more pronounced in *P. antarctica*, *T. oceanica*, and *F. cylindrus* than in *P. nitzschia antarctica*. This could be interpreted as *P. nitzschia antarctica* experiencing a lesser degree of iron stress under the same iron-deficient condition. A few additional genes, which encode proteins for adjusting under low-iron condition (Multicopper oxidase (Shaked et al., 2005), Predicted ferric reductase (Morrissey & Bowler, 2012), Putative heme iron utilization protein (Hogle et al., 2014; Hopkinson et al., 2008)), were only expressed in *P. nitzschia antarctica*. Since a few of studies observed the roles of cobalamin in the physiology of phytoplankton communities (Bertrand et al., 2007, 2015), we also analyzed the genes related cobalamin availability. Abundantly transcribed cobalamin biosynthesis protein gene in our metatranscriptomes infers that the phytoplankton communities were stressed by cobalamin-limited condition. However, we identified again that *P. nitzschia antarctica* adjust under this condition better than other taxon, which could be confirmed with higher expression

levels of methionine synthase I (cobalamin-dependent) (Ellis et al., 2017). That is, *P. nitzschia antarctica* might succeed to obtain cobalamin in the water by competing with other algal species and used it for enhancing the activity of this enzyme (Banerjee & Matthews, 1990). Thus, niche adaptation in *P. nitzschia antarctica* includes a strong ability to respond to iron-deficient condition and cobalamin-limited condition, which may be a leading cause for *P. nitzschia antarctica* dominance in the RSP phytoplankton communities. The better adjustment of *P. nitzschia antarctica* than other taxon was also detected regarding the light variation with distinctly higher photosystem II stability/assembly factor gene expression. This also infers more photosynthetic activities of *P. nitzschia antarctica* in the phytoplankton community with better acclimation to limited environmental conditions.

We further analyzed the correlation between the key-genes expression levels of *P. nitzschia antartica* and the environmental variations (Table. 6) to examine if a specific environmental factor controlled transcript abundance for a collection of genes that are involved in acclimation response to that factor. The key-genes in the functional profile of *P. nitzschia antartica* changed their overall expression patterns gradually over the sampling period; the key-gene expression levels and patterns are higher and similar in sample 5 and 6 than others (Fig. 10). The expression levels of most key-genes do not linearly correlated with the variations of major limiting factors, but might be related with general environmental parameters such as temperature, salinity or fluorescence (Table. 6). The key-genes expression patterns of *P. nitzschia antarctica* showed the potential acclimations to limited cobalamin and iron availability with abundantly transcribed genes related to these parameters (Fig. 10). Since we did not measure cobalamin

concentrations, the correlation between the cobalamin availability and the expression level of related genes could not be concluded. However, we were able to identify that the extremely low iron concentration throughout the RSP caused the higher expression of iron-related genes. We also assumed, based on the linear correlation between the cobalamin biosynthesis protein gene expression level and the iron concentrations (Table. 6), the possibility of a combination of iron and cobalamin regulating the key-genes expression patterns (Bertrand et al., 2007, 2011, 2015). We also detected the highest expression of the flavodoxin gene at station 3 although the highest dissolved iron concentration was observed at that station. This may be because the dissolved iron at the surface, supplied from sea ice melting and/or degrading of organic matters by bacterial organisms (Gerringa et al., 2015; Mack et al., 2017; Sedwick et al., 2000), had not been taken up by *P. nitzschia antarctica* when the sample was taken. Thus, the functional profiles of *P. nitzschia antarctica* showed stress from low iron conditions by expressing higher levels of flavodoxin genes, despite high iron supplies at the surface.

The genes related to carbon fixation (fructose-bisphosphate aldolase class 1 and photosystem II stability/assembly factor) inversely correlated with Photosynthetically Active Radiation (PAR) variation (Table 6). This might indicate that increased Photosynthetically Active Radiation (PAR) caused photoinhibition (van Hilst & Smith, 2002) on the photosynthetic capacity of *P. nitzschia antarctica*. In sum, we see individual species showed different acclimations to their shared environment.

CONCLUSIONS

This study demonstrates that critical environmental parameters, such as iron and light affect bulk primary production and act as stressors to the phytoplankton communities. Individual algal taxa in the phytoplankton communities showed different acclimations to their shared environmental condition, which likely determined relative abundances of each algal taxon. The phytoplankton communities during the bloom in the RSP in 2013-2014 were dominated by *P. nitzschia* sp. and acclimation of *P. nitzschia* sp. to iron and cobalamin co-limitation as well as to light variation favored this taxon. *Thalassiosira* sp. and *Phaeocystis antarctica* were stressed more severely by low iron condition than by the cobalamin limitation. Compared to these two taxa, *Fragilariopsis* sp. and *P. nitzschia* sp. displayed better adjustments to iron and cobalamin co-limitation. Acclimation to low light condition was mostly detected in *Fragilariopsis* sp. whereas acclimation to low iron conditions was observed to a higher degree in *P. nitzschia* sp. than *Fragilariopsis* sp. We also detected niche-partitioning between diatom species and the haptophyte *Phaeocystis antarctica* along depth gradients. Overall, our findings indicate that species specific traits underpin differences in acclimation responses in coexisting phytoplankton taxa.

REFERENCES

Alexander, H., Jenkins, B. D., Rynearson, T. A., & Dyhrman, S. T. (2015). Metatranscriptome analyses indicate resource partitioning between diatoms in the field. *Proceedings of the National Academy of Sciences*, *112*(17), E2182–E2190. https://doi.org/10.1073/pnas.1421993112

Armbrust, E. V. (2004). The Genome of the Diatom Thalassiosira Pseudonana: Ecology, Evolution, and Metabolism. *Science*, *306*(5693), 79–86. https://doi.org/10.1126/science.1101156

Arrigo, K. R. (1999). Phytoplankton Community Structure and the Drawdown of Nutrients and CO2 in the Southern Ocean. *Science*, *283*(5400), 365–367. https://doi.org/10.1126/science.283.5400.365

Arrigo, K. R., DiTullio, G. R., Dunbar, R. B., Robinson, D. H., VanWoert, M., Worthen, D. L., & Lizotte, M. P. (2000). Phytoplankton taxonomic variability in nutrient utilization and primary production in the Ross Sea. *Journal of Geophysical Research: Oceans*, *105*(C4), 8827–8846. https://doi.org/10.1029/1998JC000289

Arrigo, K. R., & McClain, C. R. (1994). Spring Phytoplankton Production in the Western Ross Sea. *Science*, *266*(5183), 261–263. https://doi.org/10.1126/science.266.5183.261

Arrigo, K. R., & van Dijken, G. L. (2003). Phytoplankton dynamics within 37 Antarctic coastal polynya systems. *Journal of Geophysical Research*, *108*(C8). https://doi.org/10.1029/2002JC001739

Arrigo, K. R., van Dijken, G. L., & Bushinsky, S. (2008). Primary production in the Southern Ocean, 1997–2006. *Journal of Geophysical Research*, *113*(C8). https://doi.org/10.1029/2007JC004551

Arrigo, K. R., van Dijken, G. L., & Strong, A. L. (2015). Environmental controls of marine productivity hot spots around Antarctica: PRODUCTIVITY HOT SPOTS AROUND ANTARCTICA. *Journal of Geophysical Research: Oceans*, *120*(8), 5545–5565. https://doi.org/10.1002/2015JC010888

Arrigo, K. R., van Dijken, G., & Long, M. (2008). Coastal Southern Ocean: A strong anthropogenic CO_2 sink. *Geophysical Research Letters*, *35*(21). https://doi.org/10.1029/2008GL035624

Arrigo, K. R., Worthen, D., Schnell, A., & Lizotte, M. P. (1998). Primary production in Southern Ocean waters. *Journal of Geophysical Research: Oceans*, *103*(C8), 15587–15600. https://doi.org/10.1029/98JC00930

Asper, V. L., & Smith, W. O. (1999). Particle fluxes during austral spring and summer in the southern Ross Sea, Antarctica. *Journal of Geophysical Research: Oceans*, *104*(C3), 5345–5359. https://doi.org/10.1029/1998JC900067

Banerjee, R. V., & Matthews, R. G. (1990). Cobalamin-dependent methionine synthase. *FASEB Journal: Official Publication of the Federation of American Societies for Experimental Biology*, *4*(5), 1450–1459.

Bazzaz, F. A. (1990). The Response of Natural Ecosystems to the Rising Global CO2 Levels. *Annual Review of Ecology and Systematics*, *21*(1), 167–196. https://doi.org/10.1146/annurev.es.21.110190.001123

Becquevort, S., & Smith, W. . (2001). Aggregation, sedimentation and biodegradability of phytoplankton-derived material during spring in the Ross

Sea, Antarctica. *Deep Sea Research Part II: Topical Studies in Oceanography*, *48*(19–20), 4155–4178. https://doi.org/10.1016/S0967-0645(01)00084-4

Bertrand, E. M., McCrow, J. P., Moustafa, A., Zheng, H., McQuaid, J. B., Delmont, T. O., … Allen, A. E. (2015). Phytoplankton–bacterial interactions mediate micronutrient colimitation at the coastal Antarctic sea ice edge. *Proceedings of the National Academy of Sciences*, *112*(32), 9938–9943. https://doi.org/10.1073/pnas.1501615112

Bertrand, E. M., Saito, M. A., Lee, P. A., Dunbar, R. B., Sedwick, P. N., & DiTullio, G. R. (2011). Iron Limitation of a Springtime Bacterial and Phytoplankton Community in the Ross Sea: Implications for Vitamin B12 Nutrition. *Frontiers in Microbiology*, *2*. https://doi.org/10.3389/fmicb.2011.00160

Bertrand, E. M., Saito, M. A., Rose, J. M., Riesselman, C. R., Lohan, M. C., Noble, A. E., … DiTullio, G. R. (2007). Vitamin B_{12} and iron colimitation of phytoplankton growth in the Ross Sea. *Limnology and Oceanography*, *52*(3), 1079–1093. https://doi.org/10.4319/lo.2007.52.3.1079

Bolger, A. M., Lohse, M., & Usadel, B. (2014). Trimmomatic: a flexible trimmer for Illumina sequence data. *Bioinformatics*, *30*(15), 2114–2120. https://doi.org/10.1093/bioinformatics/btu170

Boyd, P. W. (2002). ENVIRONMENTAL FACTORS CONTROLLING PHYTOPLANKTON PROCESSES IN THE SOUTHERN OCEAN1. *Journal of Phycology*, *38*(5), 844–861. https://doi.org/10.1046/j.1529-8817.2002.t01-1-01203.x

Bromwich, D. H. (1989). Satellite Analyses of Antarctic Katabatic Wind Behavior. *Bulletin of the American Meteorological Society*, *70*(7), 738–749. https://doi.org/10.1175/1520-0477(1989)070<0738:SAOAKW>2.0.CO;2

Bromwich, D. H., & Kurtz, D. D. (1984). Katabatic wind forcing of the Terra Nova Bay polynya. *Journal of Geophysical Research*, *89*(C3), 3561. https://doi.org/10.1029/JC089iC03p03561

Coale, K. H., Wang, X., Tanner, S. J., & Johnson, K. S. (2003). Phytoplankton growth and biological response to iron and zinc addition in the Ross Sea and Antarctic Circumpolar Current along 170°W. *Deep Sea Research Part II: Topical Studies in Oceanography*, *50*(3–4), 635–653. https://doi.org/10.1016/S0967-0645(02)00588-X

Cullen, J. J. (1982). The Deep Chlorophyll Maximum: Comparing Vertical Profiles of Chlorophyll *a*. *Canadian Journal of Fisheries and Aquatic Sciences*, *39*(5), 791–803. https://doi.org/10.1139/f82-108

Deibel, D., & Daly, K. L. (2007). Chapter 9 Zooplankton Processes in Arctic and Antarctic Polynyas. In *Elsevier Oceanography Series* (Vol. 74, pp. 271–322). Elsevier. Retrieved from http://linkinghub.elsevier.com/retrieve/pii/S0422989406740090

Delmont, T. O., Alderkamp, A.-C., Jenkins, B., Eren, A. M., McCrow, J. P., Bertrand, E. M., … Post, A. F. (n.d.). Manuscript: Co-occurring phytoplankton species in the Ross Sea, Antarctica, have different acclimation responses to changing light and iron levels.

Delmont, T. O., Hammar, K. M., Ducklow, H. W., Yager, P. L., & Post, A. F. (2014). Phaeocystis antarctica blooms strongly influence bacterial

community structures in the Amundsen Sea polynya. *Frontiers in Microbiology*, *5*. https://doi.org/10.3389/fmicb.2014.00646
Desjardins, P., & Conklin, D. (2010). NanoDrop Microvolume Quantitation of Nucleic Acids. *Journal of Visualized Experiments*, (1). https://doi.org/10.3791/2565
DiTullio, G. R., Grebmeier, J. M., Arrigo, K. R., Lizotte, M. P., Robinson, D. H., Leventer, A., … Dunbar, R. B. (2000). Rapid and early export of Phaeocystis antarctica blooms in the Ross Sea, Antarctica. *Nature*, *404*(6778), 595–598. https://doi.org/10.1038/35007061
DiTullio, G. R., & Smith, W. O. (1995). Relationship between dimethylsulfide and phytoplankton pigment concentrations in the Ross Sea, Antarctica. *Deep Sea Research Part I: Oceanographic Research Papers*, *42*(6), 873–892. https://doi.org/10.1016/0967-0637(95)00051-7
DiTullio, G. R., & Smith, W. O. (1996). Spatial patterns in phytoplankton biomass and pigment distributions in the Ross Sea. *Journal of Geophysical Research: Oceans*, *101*(C8), 18467–18477. https://doi.org/10.1029/96JC00034
Ellis, K. A., Cohen, N. R., Moreno, C., & Marchetti, A. (2017). Cobalamin-independent Methionine Synthase Distribution and Influence on Vitamin B12 Growth Requirements in Marine Diatoms. *Protist*, *168*(1), 32–47. https://doi.org/10.1016/j.protis.2016.10.007
El-Sayed, S. Z., Biggs, D. C., & Holm-Hansen, O. (1983). Phytoplankton standing crop, primary productivity, and near-surface nitrogenous nutrient fields in the Ross Sea, Antarctica. *Deep Sea Research Part A. Oceanographic Research Papers*, *30*(8), 871–886. https://doi.org/10.1016/0198-0149(83)90005-5
Eren, A. M., Esen, Ö. C., Quince, C., Vineis, J. H., Morrison, H. G., Sogin, M. L., & Delmont, T. O. (2015). Anvi'o: an advanced analysis and visualization platform for 'omics data. *PeerJ*, *3*, e1319. https://doi.org/10.7717/peerj.1319
Falkowski, P., & Kiefer, D. A. (1985). Chlorophyll *a* fluorescence in phytoplankton: relationship to photosynthesis and biomass. *Journal of Plankton Research*, *7*(5), 715–731. https://doi.org/10.1093/plankt/7.5.715
Fichefet, T., & Goosse, H. (1999). A numerical investigation of the spring Ross Sea polynya. *Geophysical Research Letters*, *26*(8), 1015–1018. https://doi.org/10.1029/1999GL900159
Gerringa, L. J. A., Laan, P., van Dijken, G. L., van Haren, H., De Baar, H. J. W., Arrigo, K. R., & Alderkamp, A.-C. (2015). Sources of iron in the Ross Sea Polynya in early summer. *Marine Chemistry*, *177*, 447–459. https://doi.org/10.1016/j.marchem.2015.06.002
Goffart, A., Catalano, G., & Hecq, J. . (2000). Factors controlling the distribution of diatoms and Phaeocystis in the Ross Sea. *Journal of Marine Systems*, *27*(1–3), 161–175. https://doi.org/10.1016/S0924-7963(00)00065-8
Gowing, M. M., Garrison, D. L., Kunze, H. B., & Winchell, C. J. (2001). Biological components of Ross Sea short-term particle fluxes in the austral summer of 1995–1996. *Deep Sea Research Part I: Oceanographic Research Papers*, *48*(12), 2645–2671. https://doi.org/10.1016/S0967-0637(01)00034-6
Hogle, S. L., Barbeau, K. A., & Gledhill, M. (2014). Heme in the marine environment: from cells to the iron cycle. *Metallomics*, *6*(6), 1107–1120. https://doi.org/10.1039/C4MT00031E

Hopkinson, B. M., Roe, K. L., & Barbeau, K. A. (2008). Heme Uptake by Microscilla marina and Evidence for Heme Uptake Systems in the Genomes of Diverse Marine Bacteria. *Applied and Environmental Microbiology*, *74*(20), 6263–6270. https://doi.org/10.1128/AEM.00964-08

Hutchison, G. E. (1961). The Paradox of the Plankton. *The University of Chicago Press for The American Society of Naturalists*, *XCV*(882), 137–145.

Hyatt, D., Chen, G.-L., LoCascio, P. F., Land, M. L., Larimer, F. W., & Hauser, L. J. (2010). Prodigal: prokaryotic gene recognition and translation initiation site identification. *BMC Bioinformatics*, *11*(1), 119. https://doi.org/10.1186/1471-2105-11-119

Keeling, P. J., Burki, F., Wilcox, H. M., Allam, B., Allen, E. E., Amaral-Zettler, L. A., … Worden, A. Z. (2014). The Marine Microbial Eukaryote Transcriptome Sequencing Project (MMETSP): Illuminating the Functional Diversity of Eukaryotic Life in the Oceans through Transcriptome Sequencing. *PLoS Biology*, *12*(6), e1001889. https://doi.org/10.1371/journal.pbio.1001889

Klunder, M. B., Laan, P., Middag, R., De Baar, H. J. W., & van Ooijen, J. C. (2011). Dissolved iron in the Southern Ocean (Atlantic sector). *Deep Sea Research Part II: Topical Studies in Oceanography*, *58*(25–26), 2678–2694. https://doi.org/10.1016/j.dsr2.2010.10.042

Lancelot, C., Mathot, S., Veth, C., & de Baar, H. (1993). Factors controlling phytoplankton ice-edge blooms in the marginal ice-zone of the northwestern Weddell Sea during sea ice retreat 1988: Field observations and mathematical modelling. *Polar Biology*, *13*(6), 377–387. https://doi.org/10.1007/BF01681979

Langmead, B., & Salzberg, S. L. (2012). Fast gapped-read alignment with Bowtie 2. *Nature Methods*, *9*(4), 357–359. https://doi.org/10.1038/nmeth.1923

Law, C. W., Chen, Y., Shi, W., & Smyth, G. K. (2014). voom: precision weights unlock linear model analysis tools for RNA-seq read counts. *Genome Biology*, *15*(2), R29. https://doi.org/10.1186/gb-2014-15-2-r29

Le Quere, C., Rodenbeck, C., Buitenhuis, E. T., Conway, T. J., Langenfelds, R., Gomez, A., … Heimann, M. (2007). Saturation of the Southern Ocean CO2 Sink Due to Recent Climate Change. *Science*, *316*(5832), 1735–1738. https://doi.org/10.1126/science.1136188

Lommer, M., Specht, M., Roy, A.-S., Kraemer, L., Andreson, R., Gutowska, M. A., … LaRoche, J. (2012). Genome and low-iron response of an oceanic diatom adapted to chronic iron limitation. *Genome Biology*, *13*(7), R66. https://doi.org/10.1186/gb-2012-13-7-r66

Long, S. P. (1991). Modification of the response of photosynthetic productivity to rising temperature by atmospheric CO2 concentrations: Has its importance been underestimated? *Plant, Cell and Environment*, *14*(8), 729–739. https://doi.org/10.1111/j.1365-3040.1991.tb01439.x

Mack, S. L., Dinniman, M. S., McGillicuddy, D. J., Sedwick, P. N., & Klinck, J. M. (2017). Dissolved iron transport pathways in the Ross Sea: Influence of tides and horizontal resolution in a regional ocean model. *Journal of Marine Systems*, *166*, 73–86. https://doi.org/10.1016/j.jmarsys.2016.10.008

Martin, J. H., Gordon, R. M., & Fitzwater, S. E. (1990). Iron in Antarctic waters. *Nature*, *345*(6271), 156–158. https://doi.org/10.1038/345156a0

McKay, R. M. L., Geider, R. J., & LaRoche, J. (1997). Physiological and Biochemical Response of the Photosynthetic Apparatus of Two Marine Diatoms to Fe Stress. *Plant Physiology*, *114*(2), 615–622. https://doi.org/10.1104/pp.114.2.615

McKay, R. M. L., La Roche, J., Yakunin, A. F., Durnford, D. G., & Geider, R. J. (1999). ACCUMULATION OF FERREDOXIN AND FLAVODOXIN IN A MARINE DIATOM IN RESPONSE TO FE. *Journal of Phycology*, *35*(3), 510–519. https://doi.org/10.1046/j.1529-8817.1999.3530510.x

Mock, T., Otillar, R. P., Strauss, J., McMullan, M., Paajanen, P., Schmutz, J., … Grigoriev, I. V. (2017). Evolutionary genomics of the cold-adapted diatom Fragilariopsis cylindrus. *Nature*, *541*(7638), 536–540. https://doi.org/10.1038/nature20803

Moloney, C. L., Huntley, M. E., Lopez, M. D. G., & karl, D. M. (1992). Carbon and the Antarctic Marine Food Web. *American Association for the Advancement of Science*, *257*(5067), 259–260.

Moore, J. K., & Abbott, M. R. (2000). Phytoplankton chlorophyll distributions and primary production in the Southern Ocean. *Journal of Geophysical Research: Oceans*, *105*(C12), 28709–28722. https://doi.org/10.1029/1999JC000043

Morrissey, J., & Bowler, C. (2012). Iron Utilization in Marine Cyanobacteria and Eukaryotic Algae. *Frontiers in Microbiology*, *3*. https://doi.org/10.3389/fmicb.2012.00043

Palenik, B. (2015). Molecular Mechanisms by Which Marine Phytoplankton Respond to Their Dynamic Chemical Environment. *Annual Review of Marine Science*, *7*(1), 325–340. https://doi.org/10.1146/annurev-marine-010814-015639

Parks, D. H., Tyson, G. W., Hugenholtz, P., & Beiko, R. G. (2014). STAMP: statistical analysis of taxonomic and functional profiles. *Bioinformatics*, *30*(21), 3123–3124. https://doi.org/10.1093/bioinformatics/btu494

Perovich, D. K. (1990). Theoretical estimates of light reflection and transmission by spatially complex and temporally varying sea ice covers. *Journal of Geophysical Research*, *95*(C6), 9557. https://doi.org/10.1029/JC095iC06p09557

Phipson, B., Lee, S., Majewski, I. J., Alexander, W. S., & Smyth, G. K. (2016). Robust hyperparameter estimation protects against hypervariable genes and improves power to detect differential expression. *The Annals of Applied Statistics*, *10*(2), 946–963. https://doi.org/10.1214/16-AOAS920

Redfield, A. C. (1958). The biological control of chemical factors in the environment. *Sigma Xi, The Scientific Research Society*, *46*(3), 230A, 205–221.

Ritchie, M. E., Phipson, B., Wu, D., Hu, Y., Law, C. W., Shi, W., & Smyth, G. K. (2015). limma powers differential expression analyses for RNA-sequencing and microarray studies. *Nucleic Acids Research*, *43*(7), e47–e47. https://doi.org/10.1093/nar/gkv007

Robinson, M. D., McCarthy, D. J., & Smyth, G. K. (2010). edgeR: a Bioconductor package for differential expression analysis of digital gene expression data. *Bioinformatics*, *26*(1), 139–140. https://doi.org/10.1093/bioinformatics/btp616

Robinson, M. D., & Oshlack, A. (2010). A scaling normalization method for differential expression analysis of RNA-seq data. *Genome Biology*, *11*(3), R25. https://doi.org/10.1186/gb-2010-11-3-r25

Rozema, P. D., Venables, H. J., van de Poll, W. H., Clarke, A., Meredith, M. P., & Buma, A. G. J. (2016). Interannual variability in phytoplankton biomass and species composition in northern Marguerite Bay (West Antarctic Peninsula) is governed by both winter sea ice cover and summer stratification: Changing phytoplankton at the coastal WAP. *Limnology and Oceanography*. https://doi.org/10.1002/lno.10391

Sarmiento, J. L., Hughes, T. M. C., Stouffer, R. J., & Manabe, S. (1998). Simulated response of the ocean carbon cycle to anthropogenic climate warming. *Nature*, *393*, 245–249. https://doi.org/10.1038/30455

Schlitzer, R. (2002). Carbon export fluxes in the Southern Ocean: results from inverse modeling and comparison with satellite-based estimates. *Deep Sea Research Part II: Topical Studies in Oceanography*, *49*(9–10), 1623–1644. https://doi.org/10.1016/S0967-0645(02)00004-8

Sedwick, P. N., DiTullio, G. R., & Mackey, D. J. (2000). Iron and manganese in the Ross Sea, Antarctica: Seasonal iron limitation in Antarctic shelf waters. *Journal of Geophysical Research: Oceans*, *105*(C5), 11321–11336. https://doi.org/10.1029/2000JC000256

Shaked, Y., Kustka, A. B., & Morel, F. M. M. (2005). A general kinetic model for iron acquisition by eukaryotic phytoplankton. *Limnology and Oceanography*, *50*(3), 872–882. https://doi.org/10.4319/lo.2005.50.3.0872

Shields, A. R., & Smith, W. O. (2008). An examination of the role of colonial Phaeocystis antarctica in the microbial food web of the Ross Sea. *Polar Biology*, *31*(9), 1091–1099. https://doi.org/10.1007/s00300-008-0450-z

Smith, W. O. (1995). Primary productivity and new production in the Northeast Water (Greenland) Polynya during summer 1992. *Journal of Geophysical Research*, *100*(C3), 4357. https://doi.org/10.1029/94JC02764

Smith, W. O., Ainley, D. G., Arrigo, K. R., & Dinniman, M. S. (2014). The Oceanography and Ecology of the Ross Sea. *Annual Review of Marine Science*, *6*(1), 469–487. https://doi.org/10.1146/annurev-marine-010213-135114

Smith, W. O., & Asper, V. L. (2001). The influence of phytoplankton assemblage composition on biogeochemical characteristics and cycles in the southern Ross Sea, Antarctica. *Deep Sea Research Part I: Oceanographic Research Papers*, *48*(1), 137–161. https://doi.org/10.1016/S0967-0637(00)00045-5

Smith, W. O., & Gordon, L. I. (1997). Hyperproductivity of the Ross Sea (Antarctica) polynya during austral spring. *Geophysical Research Letters*, *24*(3), 233–236. https://doi.org/10.1029/96GL03926

Smith, W. O., Marra, J., Hiscock, M. R., & Barber, R. T. (2000). The seasonal cycle of phytoplankton biomass and primary productivity in the Ross Sea, Antarctica. *Deep Sea Research Part II: Topical Studies in Oceanography*, *47*(15–16), 3119–3140. https://doi.org/10.1016/S0967-0645(00)00061-8

Smith, W. O., & Nelson, D. M. (1985). Phytoplankton Bloom Produced by a Receding Ice Edge in the Ross Sea: Spatial Coherence with the Density Field. *Science*, *227*(4683), 163–166. https://doi.org/10.1126/science.227.4683.163

Smith, W. O., Nelson, D. M., DiTullio, G. R., & Leventer, A. R. (1996). Temporal and spatial patterns in the Ross Sea: Phytoplankton biomass, elemental composition, productivity and growth rates. *Journal of Geophysical Research: Oceans*, *101*(C8), 18455–18465. https://doi.org/10.1029/96JC01304

Smith Jr., W. O., & Barber, D. G. (2007). *Polynyas: Windows to the World's Oceans* (Vol. 74). Amsterdam: Elsevier Science.

Smith Jr., W. O., & Nelson, D. M. (1986). Importance of Ice Edge Phytoplankton Production in the Southern Ocean. *Oxford University Press on Behalf of the American Institute of Biological Sciences*, *36*(4), 251–257.

Steele, J. H. (1962). ENVIRONMENTAL CONTROL OF PHOTOSYNTHESIS IN THE SEA. *Limnology and Oceanography*, *7*(2), 137–150. https://doi.org/10.4319/lo.1962.7.2.0137

Sullivan, C. W., Arrigo, K. R., McClain, C. R., Comiso, J. C., & Firestone, J. (1993). Distributions of Phytoplankton Blooms in the Southern Ocean. *Science*, *262*(5141), 1832–1837. https://doi.org/10.1126/science.262.5141.1832

Sverdrup, H. U. (1947). Wind-Driven Currents in a Baroclinic Ocean; with Application to the Equatorial Currents of the Eastern Pacific. *Proceedings of the National Academy of Sciences*, *33*(11), 318–326. https://doi.org/10.1073/pnas.33.11.318

Sweeney, C., Hansell, D. A., Carlson, C. A., Codispoti, L. ., Gordon, L. I., Marra, J., … Takahashi, T. (2000). Biogeochemical regimes, net community production and carbon export in the Ross Sea, Antarctica. *Deep Sea Research Part II: Topical Studies in Oceanography*, *47*(15–16), 3369–3394. https://doi.org/10.1016/S0967-0645(00)00072-2

Tagliabue, A., & Arrigo, K. R. (2005). Iron in the Ross Sea: 1. Impact on CO_2 fluxes via variation in phytoplankton functional group and non-Redfield stoichiometry: IRON IN THE ROSS SEA, 1. *Journal of Geophysical Research: Oceans*, *110*(C3). https://doi.org/10.1029/2004JC002531

Takahashi, T., Sutherland, S. C., Sweeney, C., Poisson, A., Metzl, N., Tilbrook, B., … Nojiri, Y. (2002). Global sea–air CO2 flux based on climatological surface ocean pCO2, and seasonal biological and temperature effects. *Deep Sea Research Part II: Topical Studies in Oceanography*, *49*(9–10), 1601–1622. https://doi.org/10.1016/S0967-0645(02)00003-6

Takahashi, T., Sutherland, S. C., Wanninkhof, R., Sweeney, C., Feely, R. A., Chipman, D. W., … de Baar, H. J. W. (2009). Climatological mean and decadal change in surface ocean pCO2, and net sea–air CO2 flux over the global oceans. *Deep Sea Research Part II: Topical Studies in Oceanography*, *56*(8–10), 554–577. https://doi.org/10.1016/j.dsr2.2008.12.009

Tatusov, R. L., Galperin, M. Y., Natale, D. A., & Koonin, E. V. (2000). The COG database: a tool for genome-scale analysis of protein functions and evolution. *Nucleic Acids Research*, *28*(1), 33–36.

Tremblay, J.-E., & Smith Jr., W. O. (2007). Phytoplankton processes in polynyas. In *Polynyas: Windows to the World's Oceans* (pp. 239–270). Amsterdam: Elsevier.

van Hilst, C. M., & Smith, W. O. (2002). Photosynthesis/irradiance relationships in the Ross Sea, Antarctica, and their control by phytoplankton assemblage

composition and environmental factors. *Marine Ecology Progress Series*, *226*, 1–12.
Wilson, D. L., Smith, W. O., & Nelson, D. M. (1986). Phytoplankton bloom dynamics of the western Ross Sea ice edge—I. Primary productivity and species-specific production. *Deep Sea Research Part A. Oceanographic Research Papers*, *33*(10), 1375–1387. https://doi.org/10.1016/0198-0149(86)90041-5
WRIGHT, S. (2008). Chemtax version 1.95 for calculating the taxonomic composition of phytoplankton populations. AU/AADC > Australian Antarctic Data Centre, Australia.
Zhu Z, Xu K, Fu F, Spackeen JL, Bronk DA, & Hutchins DA. (2016). A comparative study of iron and temperature interactive effects on diatoms and Phaeocystis antarctica from the Ross Sea, Antarctica. *Marine Ecology Progress Series*, *550*, 39–51.

TABLES

Table 1: Hydrological, physicochemical and nutrient characteristics of Ross Sea sampling sites visited during the 2013 Phantastic cruise around Western Antarctica. Abbreviations: Temp: sea surface temperature (deg C), Sal: salinity (psu), Fluor: fluorescence (AU), PAR: Photosynthetically Active Radiation (µE m^{-2} s^{-1}), Chl-*a*: chlorophyll *a* (µg L^{-1}).

Station	Depth m	Temp1 deg C	Temp2 deg C	Sal 1 psu	Sal 2 psu	Fluor AU	PAR µE m^{-2} s^{-1}
1	10	-1.08	-1.08	34.39	34.40	12.89	10.24
2	10	-0.56	-0.56	34.36	34.37	9.27	84.27
3	10	-0.71	-0.71	34.22	34.23	2.31	229.44
4	10	0.63	0.63	34.35	34.36	16.75	53.84
5	10	0.56	0.54	34.40	34.41	6.49	35.50
6	10	0.67	0.67	34.40	34.41	2.79	195.48

Station	Chl-*a* µg L^{-1}	Chl-*a* σ, µg L^{-1}	NO_2+NO_3 µM	PO_4 µM	Redfield ratio (N/P ~ 16)	Fe nM
1	5.36	0.09	19.05	1.59	12.0	0.04
2	4.22	0.12	21.22	1.47	14.4	0.04
3	2.50	0.08	19.66	1.66	11.9	0.20
4	6.51	0.06	20.70	1.12	18.5	0.05
5	3.00	0.03	19.63	1.25	15.7	0.07
6	3.12	0.06	19.50	1.27	15.3	0.06

Table 2: Characteristics of RNA extraction of water samples taken at six sampling stations in the Ross Sea during the 2013 Phantastic cruise (NBP13-10): Total volume of filtered seawater, the yield of total RNA and messenger RNA for each sample with sampling time.

Sample	Location	Vol L	date	GMT time
1	RSP	7	Dec24	8:46
2	RSP	8	Dec25	0:35
3	RSP	8	Dec27	18:48
4	RSP	4	Dec30	19:08
5	RSP	8	Jan03	18:25
6	RSP	4	Jan04	18:33
Sample	Total RNA ng/µL	mRNA ng/µL	mRNA σ, ng/µL	mRNA/Total RNA %
1	128.5	0.066	0.015	0.05
2	200.1	0.080	0.007	0.04
3	421.6	0.560	0.030	0.13
4	303.6	0.516	0.022	0.17
5	745.9	1.621	0.026	0.22
6	652.4	0.891	0.020	0.14

Table 3: The information of surveyed genomes and transcriptomes of phytoplankton species that are present in polar waters.

Reference genome	Original location	Source	
Fragilariopsis-kerguelensis-L2_C3	Southern Ocean/Antarctica	MMETSP (Thomas Mock)	Transcriptome
Fragilariopsis-kerguelensis-L26_C5	Southern Ocean	MMETSP (Andrian Marchetti)	Transcriptome
Fragilariopsis cylindrus CCMP1102	Southern Ocean	NCBI (Mock et al., 2017)	Genome
Thalassiosira-antarctica-CCMP982	Antarctica	MMETSP (Thomas Mock)	Transcriptome
Thalassiosira pseudonana CCMP1335	Moriches Bay, Long Island Sound, New York	NCBI (Armbrust et al., 2004)	Genome
Thalassiosira oceanica		NCBI (Lommer et al., 2010)	Genome
Pseudo_nitzschia-australis-10249_10_AB	Monterey Bay, Pacific	MMETSP (G Jason Smith)	Transcriptome
Pseudo_nitzschia-antarctica	Antarctica/Ross Sea Polynya	(Delmont et al., *in prep*)	Genome
Micromonas-sp-CCMP2099	Arctic/Baffin bay	MMETSP (Alexandra Z. Worden)	Transcriptome
Micromonas-sp-NEPCC29	Vancouver, Jericho Beach	MMETSP (Alexandra Z. Worden)	Transcriptome
Micromonas-sp-RCC472	Gulf of Panama, Pacific	MMETSP (Alexandra Z. Worden)	Transcriptome
Micromonas sp. ASP10-01a	Antarctica/Amundsen Sea Polynya	NCBI (Delmont et al., 2015)	Genome
Phaeocystis antarctica	Antarctica	Delmont et al., *in prep*	Transcriptome

Table 4. Total numbers of quality filtered reads of each metatranscriptome with GC content (%), and their overall local alignment rate (%) to reference genomes and transcriptomes of phytoplankton species that are present in polar waters.

Sample	1	2	3	4	5	6
Total number of filtered reads	326364	427800	31307197	27407721	29197858	23888041
%GC	48	47	48	49	48	48
Reference genome	%	%	%	%	%	%
Fragilariopsis-kerguelensis-L2_C3	21.94	10.65	6.28	6.13	3.64	5.05
Fragilariopsis-kerguelensis-L26_C5	21.46	10.25	5.98	5.79	3.36	4.73
Fragilariopsis cylindrus CCMP1102	19.61	10.1	7.05	6.9	7.06	7.97
Thalassiosira-antarctica-CCMP982	18.87	9.01	4.82	4.74	1.72	2.98
Thalassiosira pseudonana CCMP1335	15.5	7.16	3.98	4.08	1.66	2.76
Thalassiosira oceanica	17.13	7.83	4.27	4.22	1.55	2.75
Pseudo_nitzschia-australis-10249_10_AB	22.99	12.28	9.22	8.73	7.27	7.96
Pseudo_nitzschia-antarctica	35.75	34.41	46.75	42.96	73.73	66.15
Micromonas-sp-CCMP2099	12	5.75	2.92	3.02	0.82	1.59
Micromonas-sp-NEPCC29	10.82	5.29	2.7	2.85	0.82	1.48
Micromonas-sp-RCC472	12.6	5.94	2.99	3.17	1.05	1.81
Micromonas sp. ASP10-01a	0.4	0.39	0.3	0.3	0.25	0.23
Phaeocystis antarctica	0.37	0.28	0.15	0.17	0.28	0.24

Table 5: Overall local alignment (%) to selected reference genomes (Fragil: *Fragilariopsis_cylindrus* CCMP1102, Thala_oc: *Thalassiosira oceanica*, Pseudo-N: *Pseudo-nitzschia antarctica*, Phaeo: *Phaeocystis antarctica*, Micro: *Micromonas* sp. ASP10-01a).

Sample	Fragil	Thala_oc	Pseudo	Phaeo	Micro	Un-mapped	
1	64000	55906	116675	1208	1305	87270	
	19.6 %	17.1 %	35.8 %	0.4 %	0.4 %	26.7 %	100 %
2	43208	33497	147206	1198	1668	201023	
	10.1 %	7.8 %	34.4 %	0.3 %	0.4 %	47.0 %	100 %
3	2207157	1336817	14636115	46961	93922	12986225	
	7.1 %	4.3 %	46.8 %	0.2 %	0.3 %	41.5 %	100 %
4	1891133	1156606	11774357	46593	82223	12456809	
	6.9 %	4.2 %	43.0 %	0.2 %	0.3 %	45.5 %	100 %
5	2061369	452567	21527581	81754	72995	5001593	
	7.1 %	1.56 %	73.7 %	0.3 %	0.3 %	17.1 %	100 %
6	1903877	656921	15801939	57331	54942	5413030	
	8.0 %	2.8 %	66.2 %	0.2 %	0.2 %	22.7 %	100 %

Table 6: Correlation between the expression levels of key genes for acclimation responses in *Pseudo-nitzschia antarctica* and the environmental characteristics at the various sampling sites in the Ross Sea (R/A: relative abundance (%), Flu: fluorescence (AU), T: temperature (deg C), S: salinity (psu)).

Genes	Proportion	Inverse proportion
6-phosphofructokinase	Fe	chl-*a*, R/A
ABC-type Fe+- hydroxamate transport system		N
ABC-type transport system involved in Fe-S cluster assembly, permease and ATPase components		Flu
Cobalamin biosynthesis protein CobN, Mg-chelatase	Fe, P	chl-*a*, R/A
Cytochrome c biogenesis protein CcdA		Flu
Deoxyribodipyrimidine photolyase	T, S	Flu
Ferredoxin-NADP reductase	T, S	Flu
Predicted ferric reductase Ca2+binding protein, EF-hand superfamily		Flu
Flavodoxin		Flu
Fructose-bisphosphate aldolase class 1		PAR/irradiance
Methionine synthase I (cobalamin-dependant)		Flu
Mg-chelatase subunit ChlD		T, S
Multicopper oxidase with three cupredoxin domains		N
NADPH-dependent glutamate synthase beta chain	T, S	
Photosystem II stability/assembly factor		PAR/irradiance
Putative heme iron utilization protein		Flu

FIGURE LEGENDS

Figure 1: Sampling sites in the RSP during the NBP13-10 cruise in the austral spring-summer (Dec 24. 2013 – Jan 4. 2014).

Figure 2: Surface chl-*a* concentration and the status of sea ice cover in the RSP during the sampling period (Dec 24. 2013 – Jan 04. 2014).

Figure 3: The inverse correlation between Photosynthetically Active Radiation (PAR) and fluorescence (panel a), and between Photosynthetically Active Radiation (PAR) and chl-*a* concentrations (panel b).

Figure 4: Calculated TPM (transcripts per million) of mapped reads to five reference genomes (panel a), relative abundance of each algal species determined by FlowCAM data (panel b), relative abundance of each algal species determined by HPLC pigment analysis (panel c).

Figure 5: Calculated TPM (transcripts per million) of mapped reads to three diatom species genomes (panel a), and relative abundance of *Pseudo-nitzschia* sp., *Thalassisosira* sp., and *Fragilariopsis* sp. determined by 18S diatom community data (Filliger, unpublished) (panel b).

Figure 6: The distribution of mapped reads on the reference genomes. The most inner circle presents the reference genomes (contigs with GC content). The black lines of each circle (each sample) indicate the coverage of each contig of the reference genomes. The bar graphs indicate the library sizes. (a) *Phaeocystis antarctica*, (b) *Fragilariopsis cylindrus*, (c) *Pseudo-nitzschia antarctica*, (d) *Thalassiosira oceanica*, and (e) *Micromonas* sp. ASP 10-01.

Figure 7: The differences in the global gene expression patterns of each reference species across the stations 3, 4, 5 and 6. (a) *Phaeocystis antarctica*, (b)

Fragilariopsis cylindrus, (c) *Pseudo-nitzschia antarctica*, (d) *Thalassiosira oceanica*, and (e) *Micromonas* sp. ASP 10-01.

Figure 8: Heat maps of transcript abundance for key-genes that encode acclimation response in each reference species across all samples. Transcripts for genes to together code a single protein complex were merged.

Figure 9: Heat maps of normalized transcript abundance in a log2 scale, for key-genes in each reference species across the sample 3, 4, 5, and 6. Transcripts for genes to together code single protein complex were merged.

Figure 10: Heat map of normalized transcript abundance in a log2 scale, for key-gene expression in *Pseudo-nitzschia antarctica* across the sample3, 4, 5, and 6. The genes are arranged in descending order of mean gene expression level of four samples.

Figure 1.

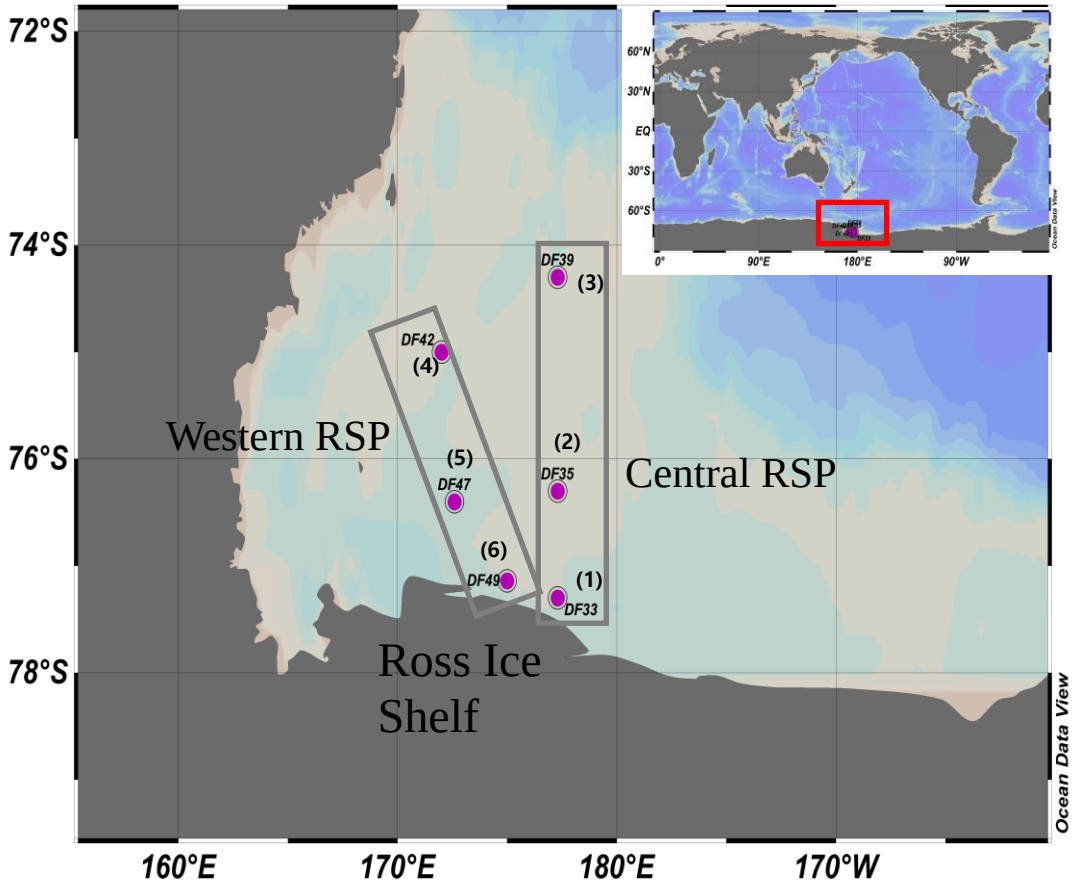
72°S
74°S
76°S
78°S
160°E
170°E
180°E
170°W
60°N
30°N
EQ
30°S
60°S
0°
90°E
180°E
90°W
DF39
(3)
DF42
(4)
Western RSP
(2)
(5)
DF35
DF47
Central RSP
(6)
DF49
(1)
DF33
Ross Ice
Shelf
Ocean Data View

Figure 2.

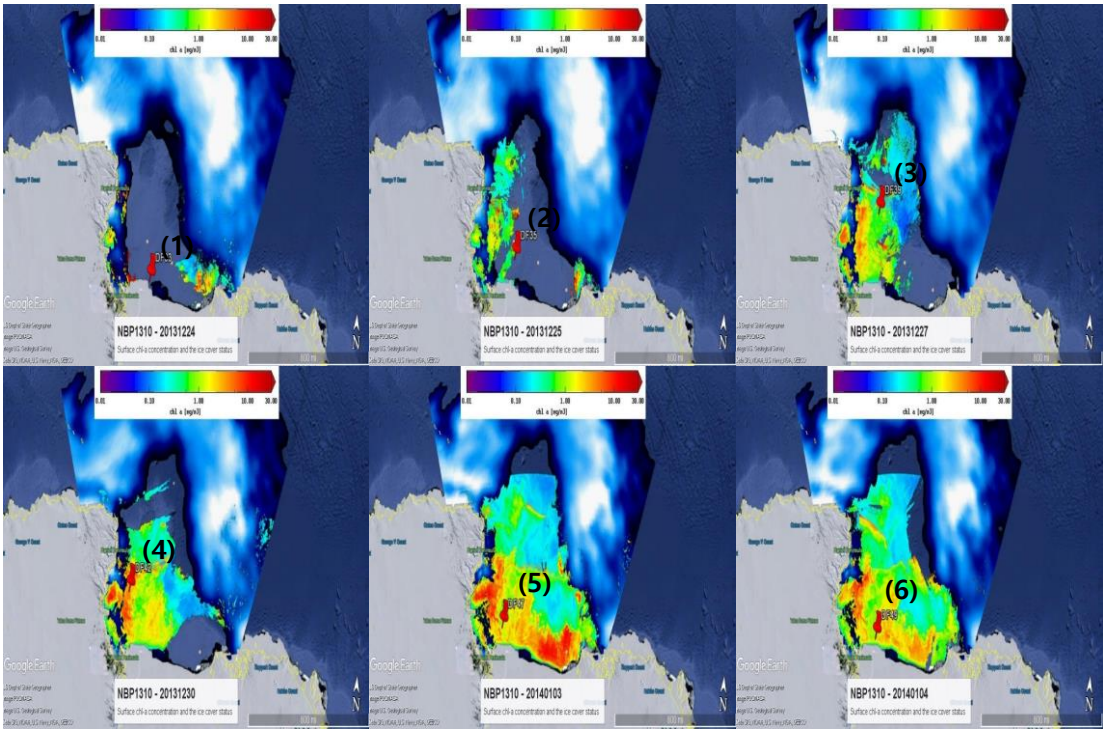
(1)
NBP1310 - 20131224
(2)
NBP1310 - 20131225
(3)
NBP1310 - 20131227
(4)
NBP1310 - 20131230
(5)
NBP1310 - 20140103
(6)
NBP1310 - 20140104

Figure 3.

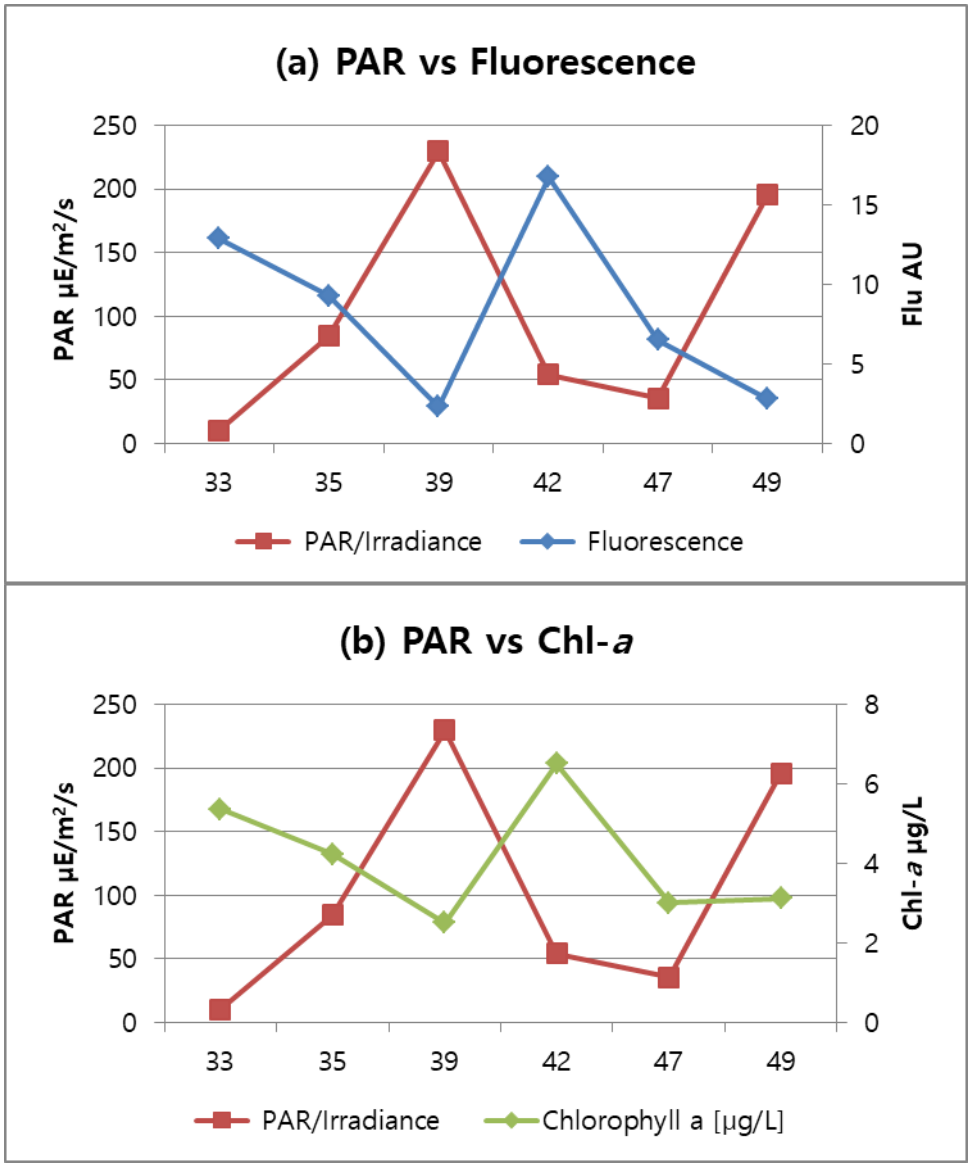
(a) PAR vs Fluorescence
PAR µE/m²/s
Flu AU
250
200
150
100
50
0
20
15
10
5
0
33
35
39
42
47
49
PAR/Irradiance
Fluorescence
(b) PAR vs Chl-a
PAR µE/m²/s
Chl-a µg/L
250
200
150
100
50
0
8
6
4
2
0
33
35
39
42
47
49
PAR/Irradiance
Chlorophyll a [µg/L]

Figure 4.

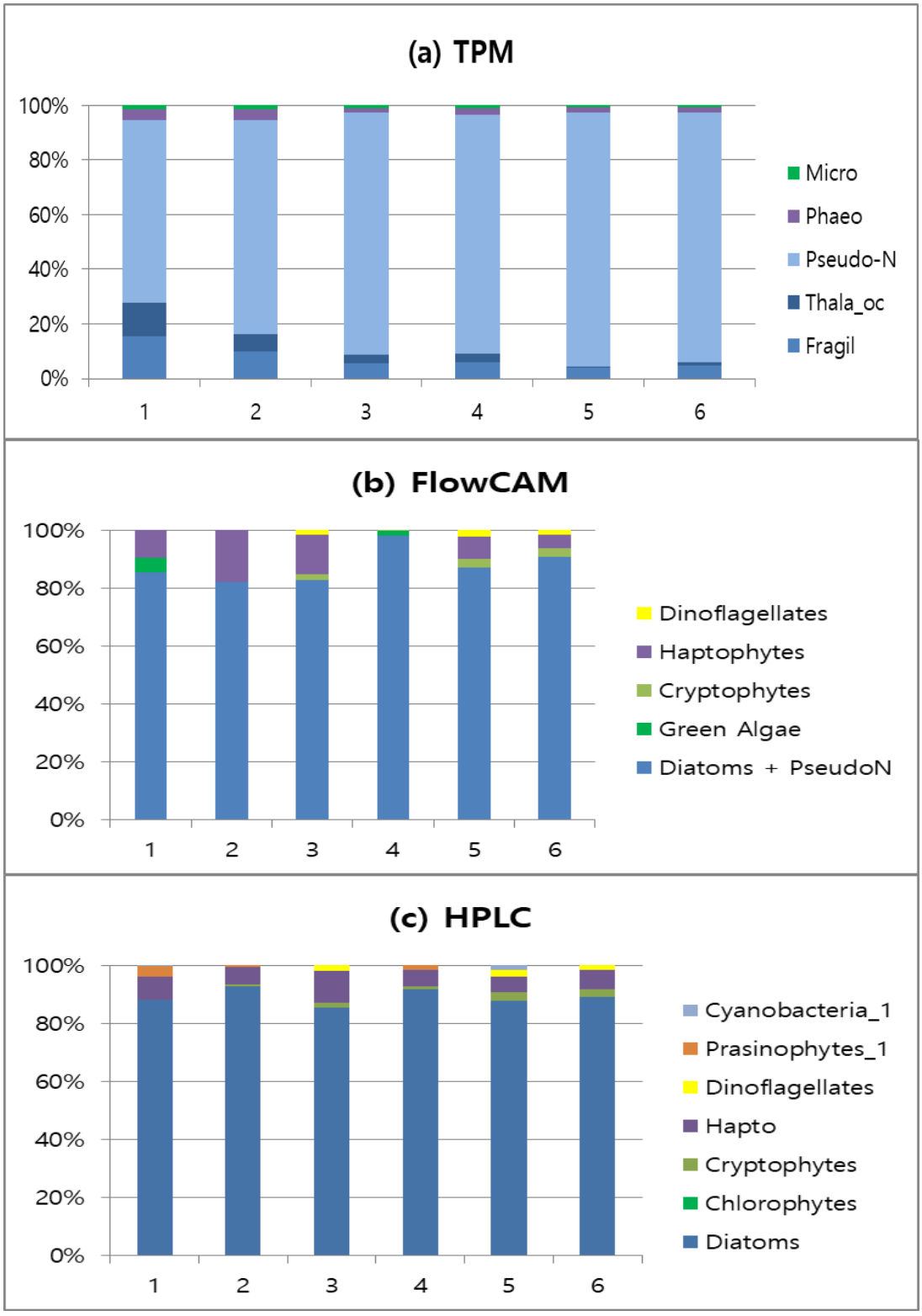
(a) TPM
100%
80%
60%
40%
20%
0%
1
2
3
4
5
6
Micro
Phaeo
Pseudo-N
Thala_oc
Fragil
(b) FlowCAM
100%
80%
60%
40%
20%
0%
1
2
3
4
5
6
Dinoflagellates
Haptophytes
Cryptophytes
Green Algae
Diatoms + PseudoN
(c) HPLC
100%
80%
60%
40%
20%
0%
1
2
3
4
5
6
Cyanobacteria_1
Prasinophytes_1
Dinoflagellates
Hapto
Cryptophytes
Chlorophytes
Diatoms

Figure 5.

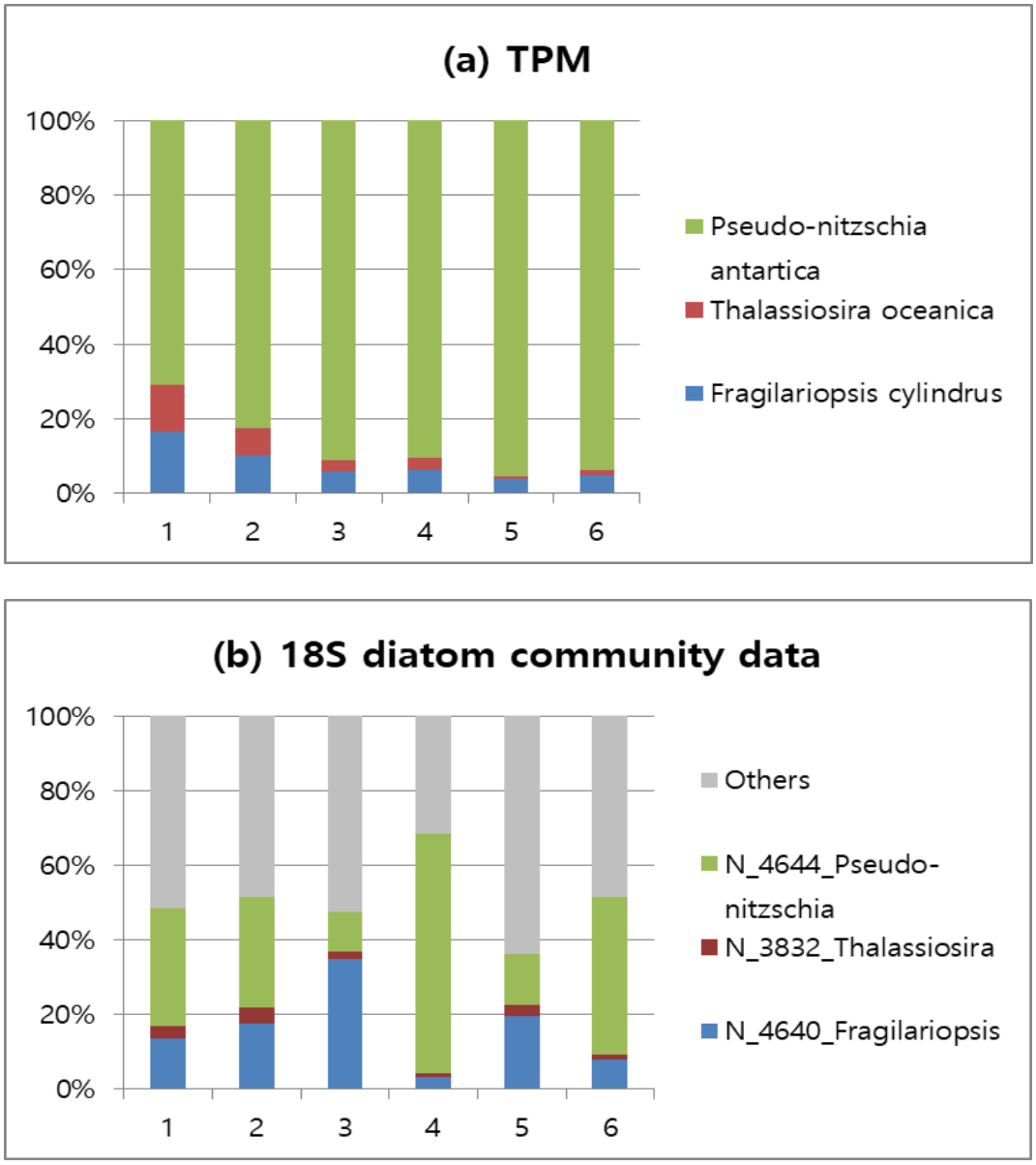
(a) TPM
100%
80%
60%
40%
20%
0%
1
2
3
4
5
6
Pseudo-nitzschia antartica
Thalassiosira oceanica
Fragilariopsis cylindrus
(b) 18S diatom community data
100%
80%
60%
40%
20%
0%
1
2
3
4
5
6
Others
N_4644_Pseudo-nitzschia
N_3832_Thalassiosira
N_4640_Fragilariopsis

Figure 6. (a) and (b)

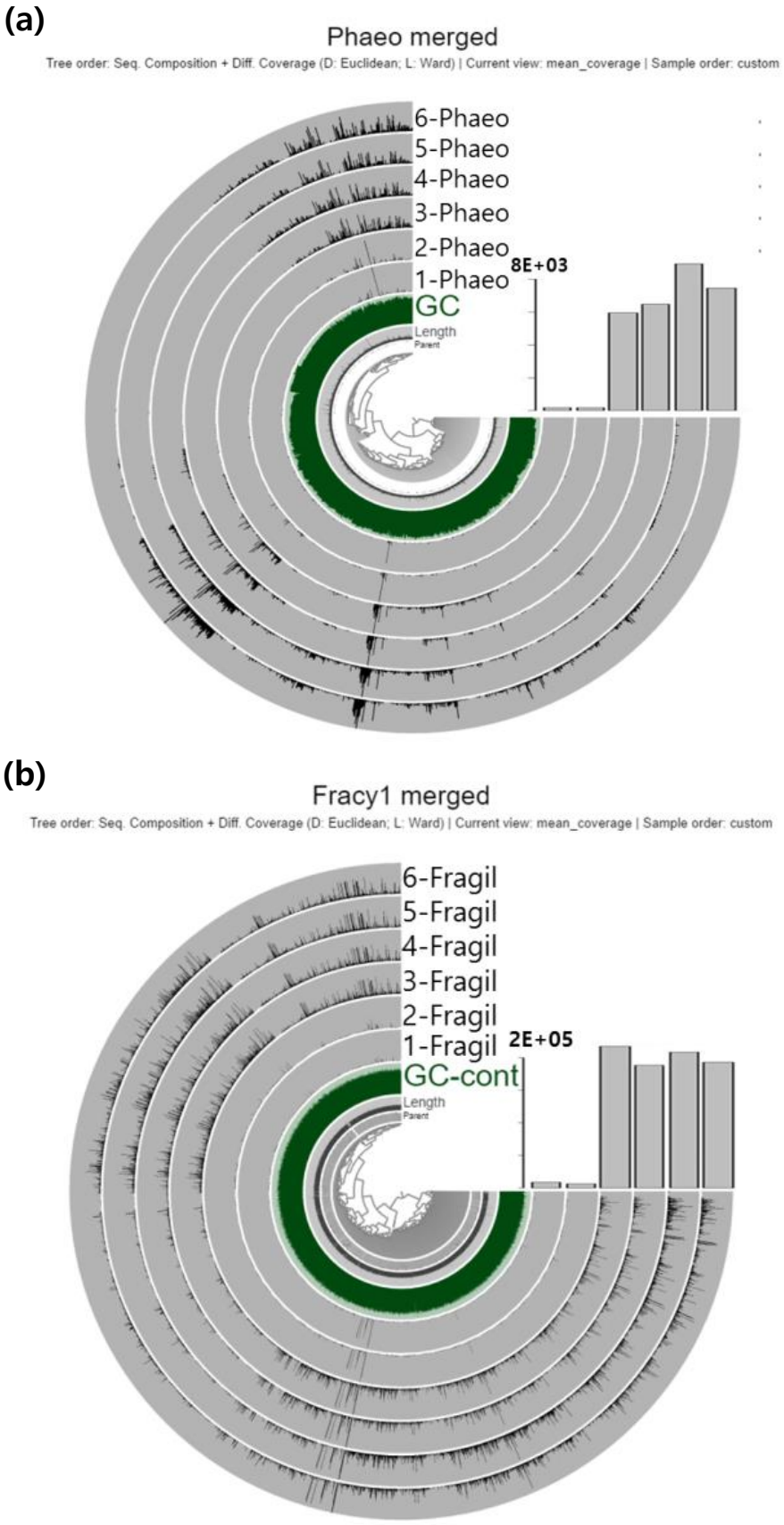

Figure 6. (c) and (d)

(c)

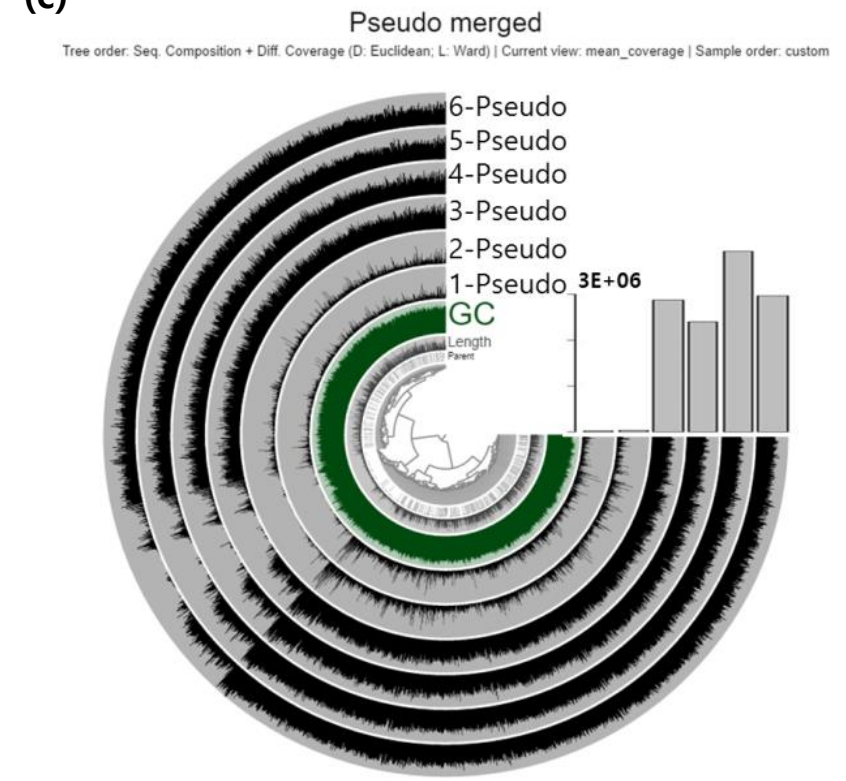

(d)

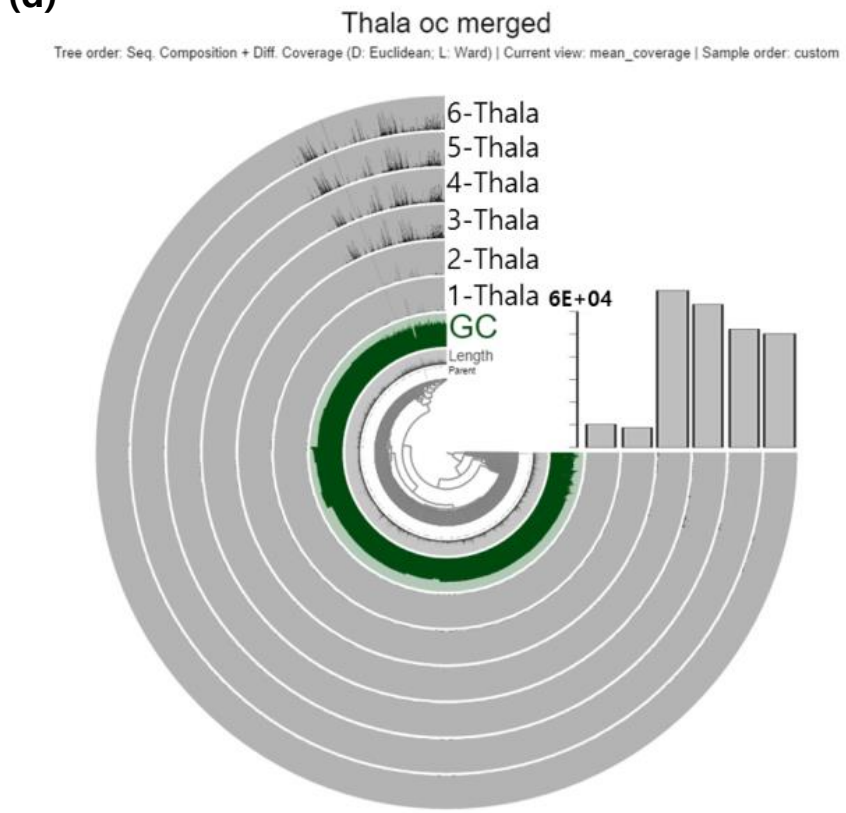

Figure 6. (e)

(e)

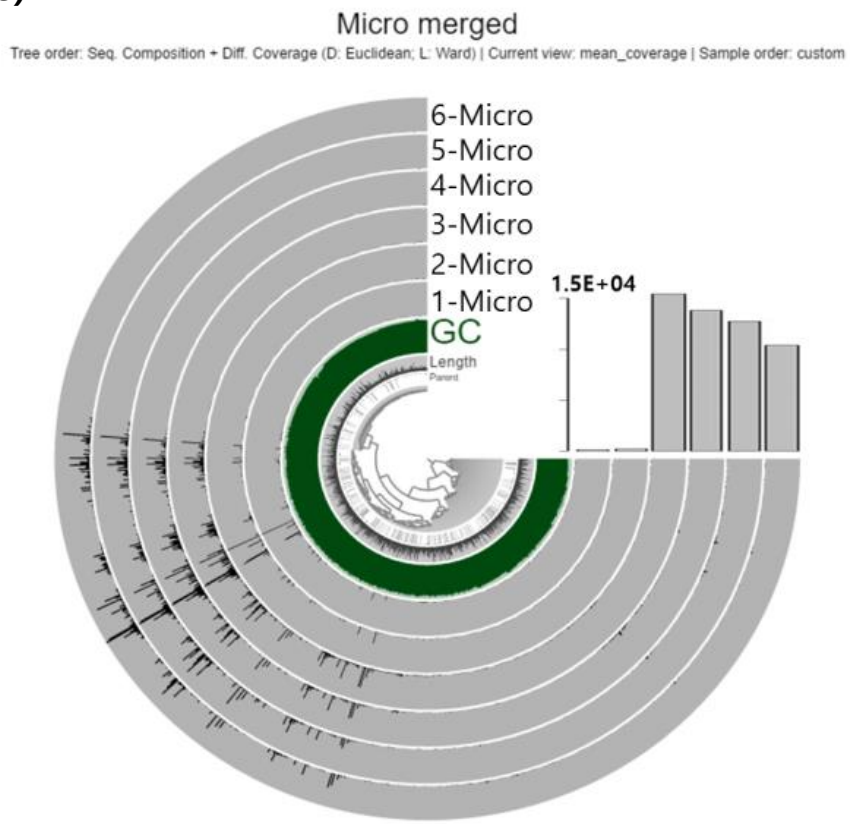
Micro merged
Tree order: Seq. Composition + Diff. Coverage (D: Euclidean; L: Ward) | Current view: mean_coverage | Sample order: custom
6-Micro
5-Micro
4-Micro
3-Micro
2-Micro
1-Micro
GC
Length
Parent
1.5E+04

Figure 7.

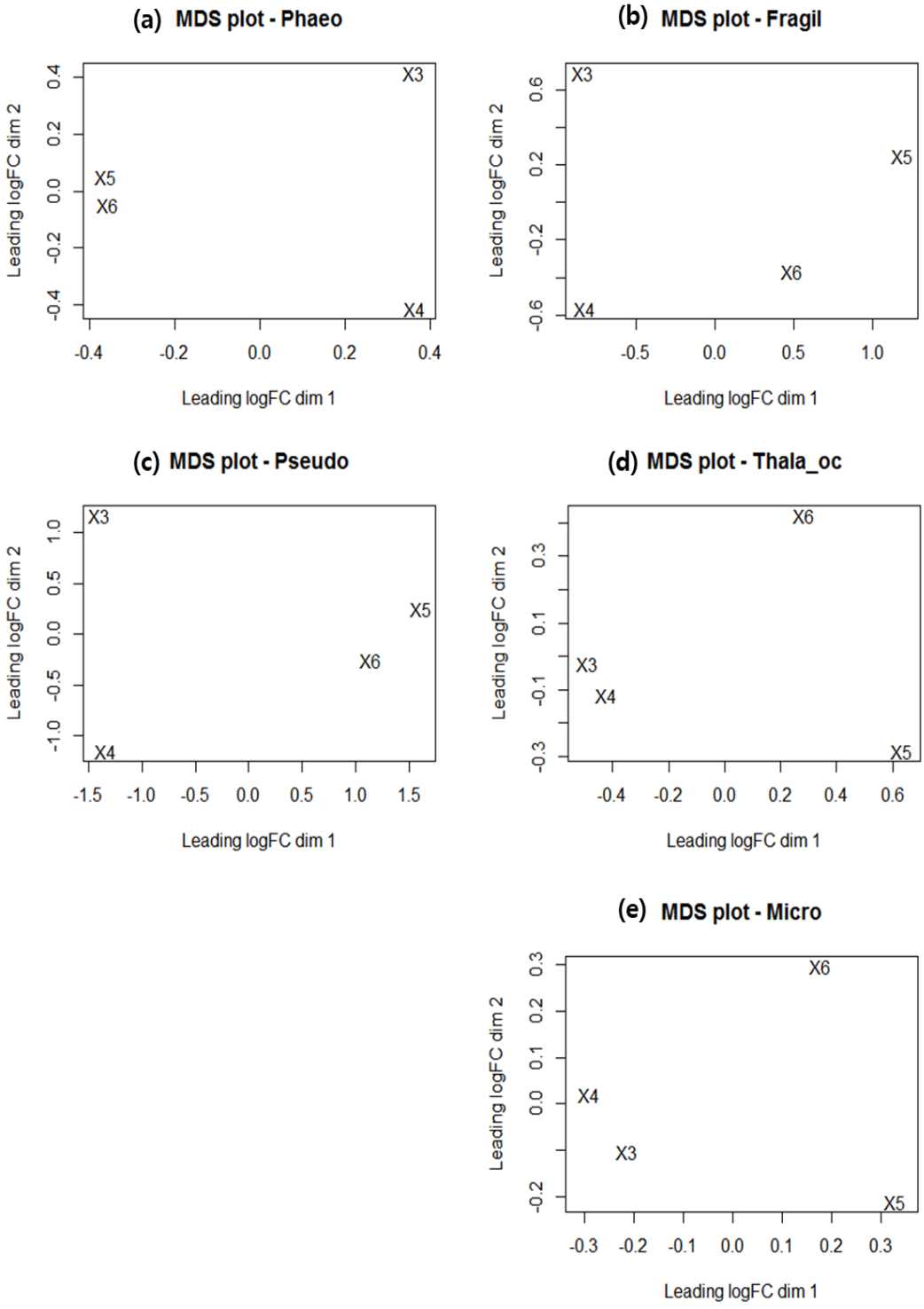
(a) MDS plot - Phaeo
X3
X5
X6
X4
Leading logFC dim 2
Leading logFC dim 1
(b) MDS plot - Fragil
X3
X5
X6
X4
Leading logFC dim 2
Leading logFC dim 1
(c) MDS plot - Pseudo
X3
X5
X6
X4
Leading logFC dim 2
Leading logFC dim 1
(d) MDS plot - Thala_oc
X6
X3
X4
X5
Leading logFC dim 2
Leading logFC dim 1
(e) MDS plot - Micro
X6
X4
X3
X5
Leading logFC dim 2
Leading logFC dim 1

Figure 8.

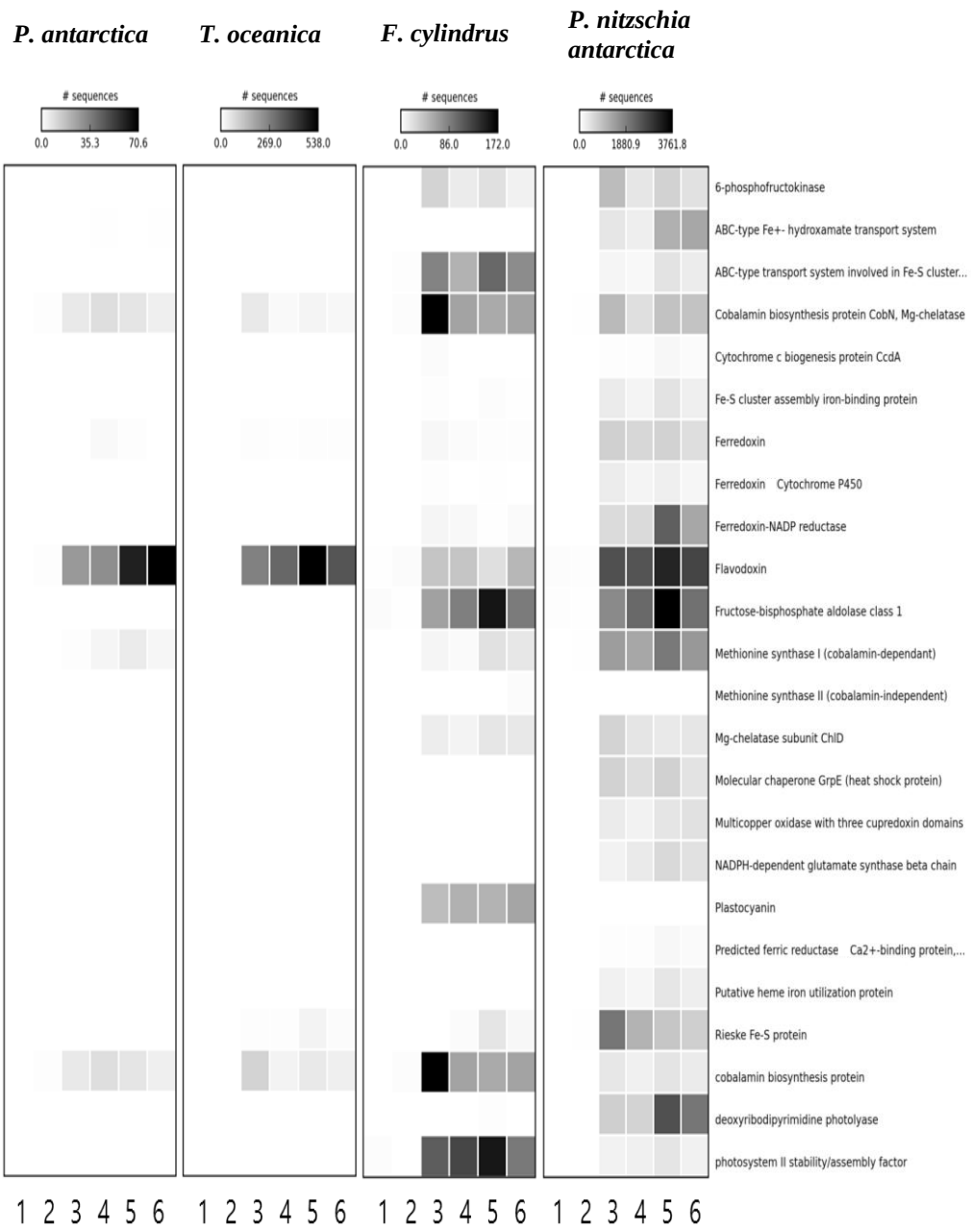
P. antarctica
T. oceanica
F. cylindrus
P. nitzschia antarctica
sequences
0.0 35.3 70.6
0.0 269.0 538.0
0.0 86.0 172.0
0.0 1880.9 3761.8
6-phosphofructokinase
ABC-type Fe+- hydroxamate transport system
ABC-type transport system involved in Fe-S cluster...
Cobalamin biosynthesis protein CobN, Mg-chelatase
Cytochrome c biogenesis protein CcdA
Fe-S cluster assembly iron-binding protein
Ferredoxin
Ferredoxin Cytochrome P450
Ferredoxin-NADP reductase
Flavodoxin
Fructose-bisphosphate aldolase class 1
Methionine synthase I (cobalamin-dependant)
Methionine synthase II (cobalamin-independent)
Mg-chelatase subunit ChlD
Molecular chaperone GrpE (heat shock protein)
Multicopper oxidase with three cupredoxin domains
NADPH-dependent glutamate synthase beta chain
Plastocyanin
Predicted ferric reductase Ca2+-binding protein,...
Putative heme iron utilization protein
Rieske Fe-S protein
cobalamin biosynthesis protein
deoxyribodipyrimidine photolyase
photosystem II stability/assembly factor
1 2 3 4 5 6 1 2 3 4 5 6 1 2 3 4 5 6 1 2 3 4 5 6

Figure 9.

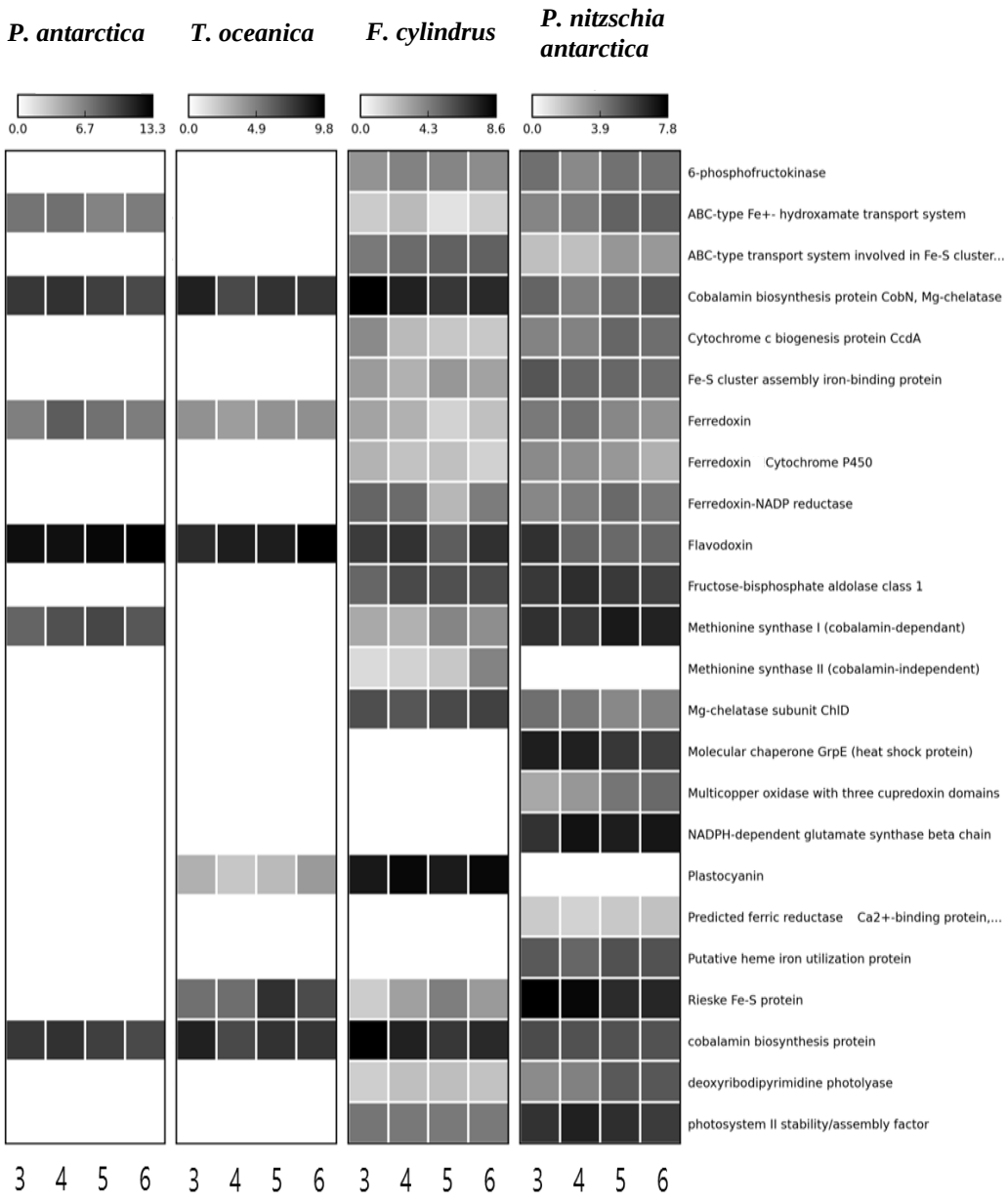
P. antarctica
T. oceanica
F. cylindrus
P. nitzschia antarctica
0.0 6.7 13.3
0.0 4.9 9.8
0.0 4.3 8.6
0.0 3.9 7.8
6-phosphofructokinase
ABC-type Fe+- hydroxamate transport system
ABC-type transport system involved in Fe-S cluster...
Cobalamin biosynthesis protein CobN, Mg-chelatase
Cytochrome c biogenesis protein CcdA
Fe-S cluster assembly iron-binding protein
Ferredoxin
Ferredoxin Cytochrome P450
Ferredoxin-NADP reductase
Flavodoxin
Fructose-bisphosphate aldolase class 1
Methionine synthase I (cobalamin-dependant)
Methionine synthase II (cobalamin-independent)
Mg-chelatase subunit ChlD
Molecular chaperone GrpE (heat shock protein)
Multicopper oxidase with three cupredoxin domains
NADPH-dependent glutamate synthase beta chain
Plastocyanin
Predicted ferric reductase Ca2+-binding protein,...
Putative heme iron utilization protein
Rieske Fe-S protein
cobalamin biosynthesis protein
deoxyribodipyrimidine photolyase
photosystem II stability/assembly factor
3 4 5 6 3 4 5 6 3 4 5 6 3 4 5 6

Figure 10.

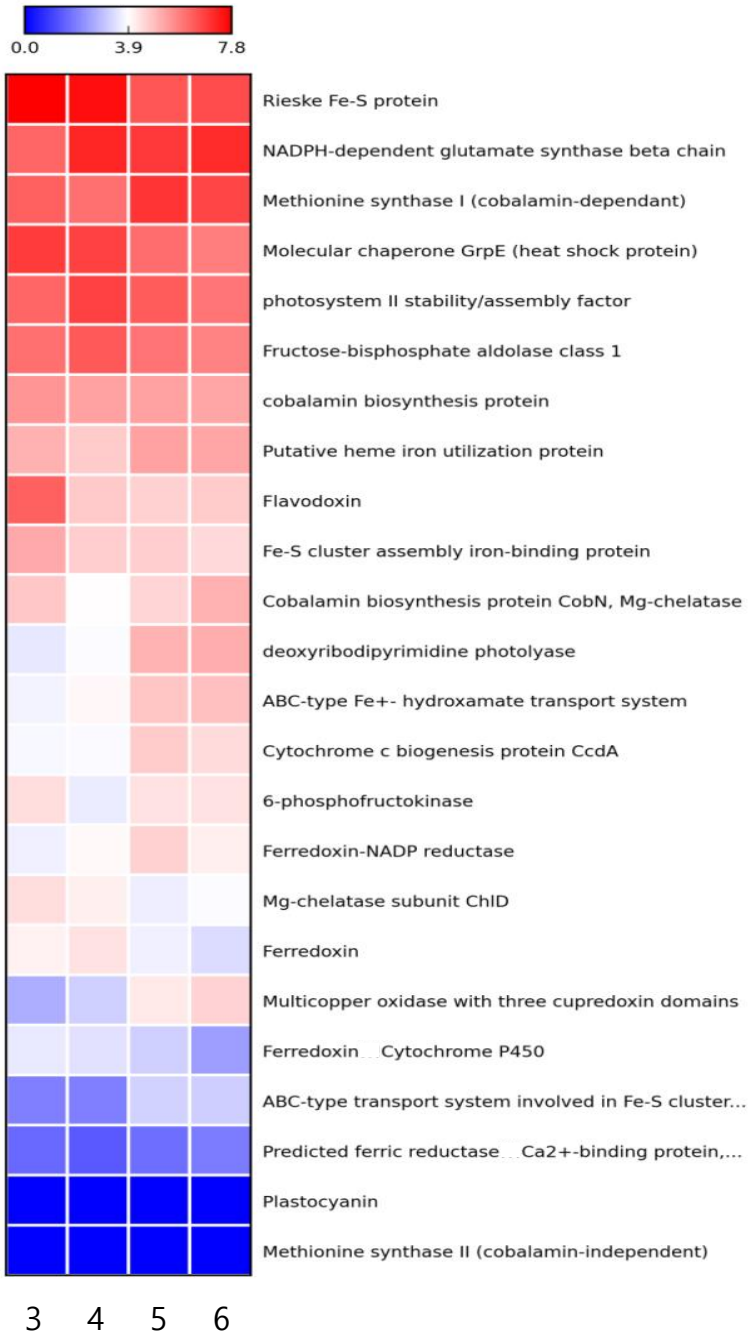
0.0
3.9
7.8
Rieske Fe-S protein
NADPH-dependent glutamate synthase beta chain
Methionine synthase I (cobalamin-dependant)
Molecular chaperone GrpE (heat shock protein)
photosystem II stability/assembly factor
Fructose-bisphosphate aldolase class 1
cobalamin biosynthesis protein
Putative heme iron utilization protein
Flavodoxin
Fe-S cluster assembly iron-binding protein
Cobalamin biosynthesis protein CobN, Mg-chelatase
deoxyribodipyrimidine photolyase
ABC-type Fe+- hydroxamate transport system
Cytochrome c biogenesis protein CcdA
6-phosphofructokinase
Ferredoxin-NADP reductase
Mg-chelatase subunit ChlD
Ferredoxin
Multicopper oxidase with three cupredoxin domains
Ferredoxin Cytochrome P450
ABC-type transport system involved in Fe-S cluster...
Predicted ferric reductase Ca2+-binding protein,...
Plastocyanin
Methionine synthase II (cobalamin-independent)
3
4
5
6

APPENDICES FIGURE LEGENDS

Appendix 1: Multidimensional plots of each reference genome species showing how different the global gene expression patterns are across the sampling sites. We found that the extremely low library sizes of samples 1 and 2 compared to the rest caused a significant bias. (a) *Phaeocystis antarctica*, (b) *Fragilariopsis cylindrus*, (c) *Pseudo-nitzschia antarctica*, (d): *Thalassiosira oceanica*, and (e) *Micromonas* sp. ASP 10-01.

Appendix 2: The vertical profile of relative abundances of diatoms and haptophytes determined by FlowCAM data at the sampling sites.

Appendix 1.

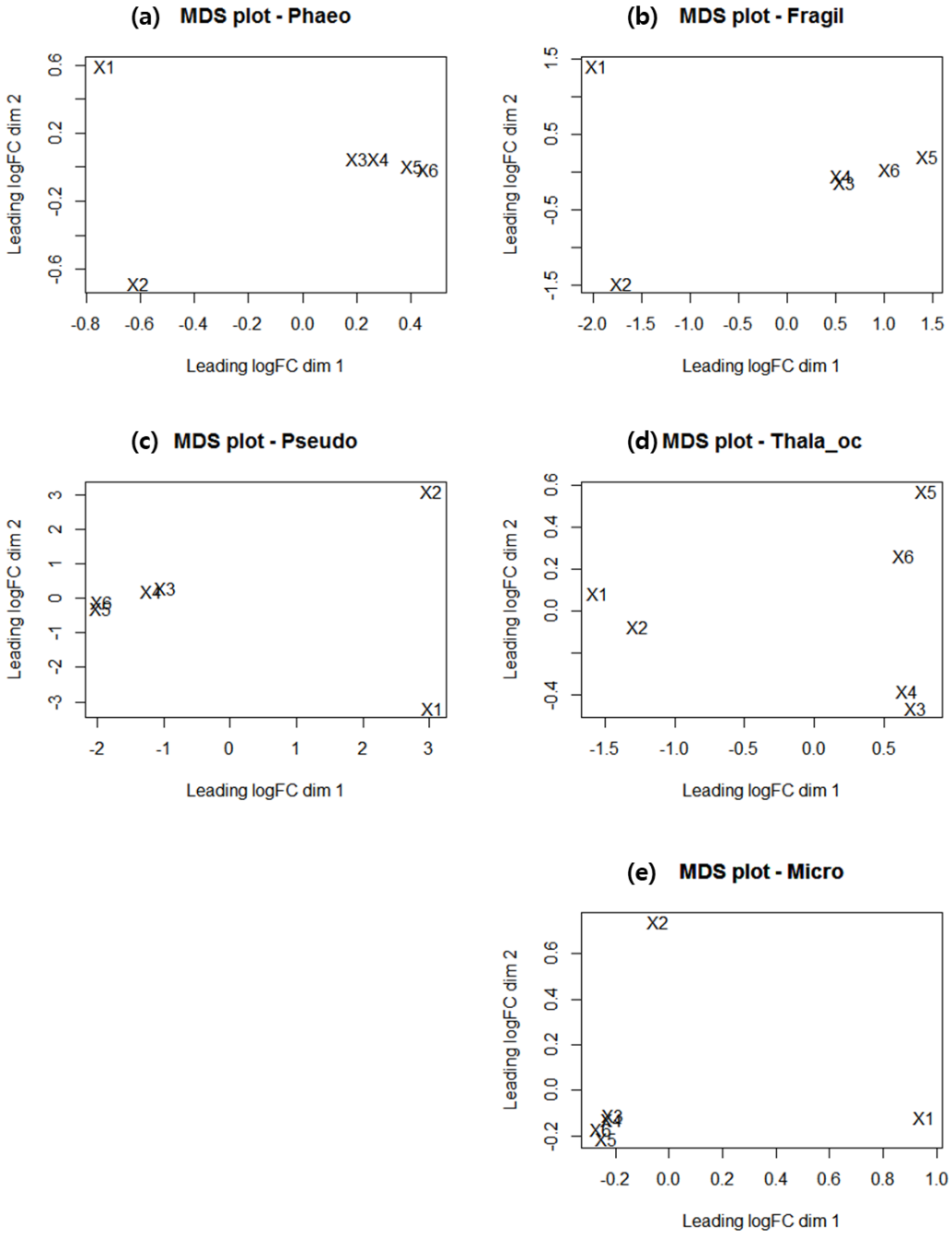
(a) MDS plot - Phaeo
Leading logFC dim 2
Leading logFC dim 1
X1
X2
X3X4
X5
X6
(b) MDS plot - Fragil
Leading logFC dim 2
Leading logFC dim 1
X1
X2
X3
X4
X5
X6
(c) MDS plot - Pseudo
Leading logFC dim 2
Leading logFC dim 1
X1
X2
X3
X4
X5
X6
(d) MDS plot - Thala_oc
Leading logFC dim 2
Leading logFC dim 1
X1
X2
X3
X4
X5
X6
(e) MDS plot - Micro
Leading logFC dim 2
Leading logFC dim 1
X1
X2

Appendix 2.